

# 1 Crystal and volatile controls on the mixing and mingling of magmas

2

3 P. A. Jarvis <sup>1</sup>, M. Pistone <sup>2,3</sup>, A. Secretan <sup>2</sup>, J. D. Blundy <sup>4</sup>, K. V. Cashman <sup>4</sup>, H. M.  
4 Mader <sup>4</sup>, L. P. Baumgartner <sup>2</sup>

5 <sup>1</sup> Section of Earth and Environmental Sciences, University of Geneva, Geneva, Switzerland

6 <sup>2</sup> Institute of Earth Sciences, University of Lausanne (UNIL), Lausanne, Switzerland

7 <sup>3</sup> Department of Geology, Franklin College of Arts and Sciences, University of Georgia,  
8 Athens, USA

9 <sup>4</sup> School of Earth Sciences, University of Bristol, Bristol, United Kingdom

10

11 **Keywords:** Magma mixing. Magma mingling, Multi-phase modelling, Petrographic observa-  
12 tions

13

## 14 **Abstract**

15 The mixing and mingling of magmas of different compositions are important geological pro-  
16 cesses. They produce various distinctive textures and geochemical signals in both plutonic  
17 and volcanic rocks and have implications for eruption triggering. Both processes are widely  
18 studied, with prior work focusing on field and textural observations, geochemical analysis of  
19 samples, theoretical and numerical modelling, and experiments. However, despite the vast  
20 amount of existing literature, there remain numerous unresolved questions. In particular, how  
21 does the presence of crystals and exsolved volatiles control the dynamics of mixing and min-  
22 gling? Furthermore, to what extent can this dependence be parameterised through the effect  
23 of crystallinity and vesicularity on bulk magma properties such as viscosity and density? In  
24 this contribution, we review the state of the art for models of mixing and mingling processes  
25 and how they have been informed by field, analytical, experimental and numerical investiga-  
26 tions. We then show how analytical observations of mixed and mingled lavas from four vol-  
27 canoes (Chaos Crags, Lassen Peak, Mt. Unzen and Soufrière Hills) have been used to infer a  
28 conceptual model for mixing and mingling dynamics in magma storage regions. Finally, we  
29 review recent advances in incorporating multi-phase effects in numerical modelling of mix-  
30 ing and mingling, and highlight the challenges associated with bringing together empirical  
31 conceptual models and theoretically-based numerical simulations.

32

33 **1 Introduction: Magma mixing and mingling and volcanic plumbing systems**

34 It is now widely accepted that magmas of different compositions can mix and mingle together  
35 (Blake et al., 1965; Eichelberger, 1980; Sparks & Marshall, 1986; Wiebe, 1987; Snyder,  
36 1997; Wilcox, 1999; Perugini & Poli, 2012; Morgavi et al., 2019). Textural consequences of  
37 mingling have long been observed (Phillips, 1880; Judd, 1893) although the earliest observa-  
38 tions were not necessarily interpreted correctly (Wilcox, 1999), with heterogeneities inter-  
39 preted as originating from metasomatism (Fenner, 1926) or solid-state diffusion (Nockolds,  
40 1933). Advancements in geochemical analysis combined with an understanding of phase  
41 equilibria led to acknowledgement of mixing and mingling as key processes, alongside crys-  
42 tal fractionation, in producing the compositional diversity of igneous rocks (Vogel et al.,  
43 2008). Additionally, interaction between magmas became recognised as a potential trigger for  
44 volcanic eruptions (Sparks et al., 1977). Evidently, understanding mixing and mingling pro-  
45 cesses is crucial for deciphering the evolution of igneous rocks and the eruptive dynamics of  
46 volcanoes.

47

48 Previous work has sometimes been flexible with regards to precise definitions of the terms  
49 ‘mixing’ and ‘mingling’. We here define mixing to be chemical interaction between two  
50 magmas that produces a composition intermediate between the original end-members (Bun-  
51 sen, 1851). Chemical mixing proceeds by chemical diffusion (Watson, 1982; Leshner, 1994)  
52 and, if allowed to complete, leads to hybridisation and homogeneous products (Humphreys et  
53 al., 2010). By contrast, mingling is the physical interaction of the two magmas, such as  
54 through convective stirring (e.g., Oldenburg et al., 1989) or chaotic advection (e.g., Perugini  
55 & Poli, 2004; Morgavi et al., 2013), and creates compositional heterogeneities. Mixing and  
56 mingling often occur together, with mixing acting to ‘smooth-out’ compositional heterogene-  
57 ities produced by mingling. However, mixing and mingling can be inhibited by large con-  
58 trasts in magma viscosity (Sparks & Marshall, 1986; Frost & Mahood, 1987; Sato & Sato,  
59 2009) and density (Blake & Fink, 1987; Koyaguchi & Blake, 1989; Grasset & Albarade,  
60 1994). If homogenisation is sufficiently slow then cooling and/or degassing of the system can  
61 lead to crystallisation and preservation of a variety of textural and chemical signatures  
62 (D’Lemos, 1987; Morgavi et al., 2016) reflecting the temperatures, compositions, crystallini-  
63 ties and relative proportions of the initial magmas (Eichelberger, 1980; Bacon, 1986; Sparks  
64 & Marshall, 1986).

65

66 Mixing and mingling models typically assume injection of a hotter, mafic magma into a  
67 cooler, more felsic host (Campbell & Turner, 1989; Clyne, 1999). This can be followed by

68 later intrusion (or back-injection) of veins and pipes of remobilised felsic material into the  
69 mafic component (Elwell et al., 1960; 1962; Wiebe, 1992; 1994; 1996; Wiebe & Collins,  
70 1998; Wiebe et al., 2002; Wiebe & Hawkins, 2015). Such injections have been modelled ex-  
71 perimentally (Huppert et al., 1984, 1986; Campbell & Turner, 1986; Snyder & Tait, 1995;  
72 Perugini & Poli, 2005), theoretically (Sparks & Marshall, 1986) and numerically (Andrews &  
73 Manga, 2014; Montagna et al., 2015). Additionally, heat and volatile transfer from the mafic  
74 to the felsic end-member induces physico-chemical responses in both magmas. The mafic  
75 component undergoes crystallisation and degassing due to undercooling (Eichelberger, 1980;  
76 Cashman & Blundy, 2000; Coombs et al., 2002; Petrelli et al., 2018), leading to an increase  
77 in bulk viscosity (Caricchi et al., 2007; Mader et al., 2013) and potentially a decrease in den-  
78 sity (if bubbles of the exsolved gas phase remains trapped), whereas the felsic magma par-  
79 tially melts due to super-heating (Pistone et al., 2017). This can create a temporal window  
80 where the bulk viscosities of the two magmas become closer thereby facilitating mingling  
81 and mixing before continued crystallisation of the mafic magma increases its viscosity. An-  
82 other scenario is mixing and mingling between partially-molten silicic rocks and a hot, rhyo-  
83 litic injection (Bindeman and Simakin, 2014), which is important for the formation of large,  
84 eruptible magma bodies containing crystals mixed from different portions of the same magma  
85 storage system (antecrysts; Francalanci et al., 2011; Ubide et al., 2014; Stelten et al., 2015;  
86 Bindeman & Melnik, 2016; Seitz et al., 2018). In all cases, the physico-chemical changes and  
87 their associated timescales govern the style of mixing, the resultant textures and the eruptive  
88 potential.

89

### 90 *1.1 Chemical mixing*

91 Chemical mixing occurs through the diffusion of different components along spatial gradients  
92 in chemical potential (Adkins, 1983) to create homogeneous products. If all components have  
93 equal diffusivities, the mixing of two chemically-distinct magmas gives rise to linear trends  
94 on Harker-type variation diagrams (Harker, 1909) that can be used to constrain the end-mem-  
95 ber compositions. Non-linear mixing trends produced by variable diffusivities amongst melt  
96 components, including trace elements (Nakamura & Kushiro, 1998; Perugini et al., 2008; Pe-  
97 rugini et al., 2013), are also common and have been identified in various localities (Reid et  
98 al., 1983; Bacon & Metz, 1984; Cantagrel et al., 1984; Gourgaud & Maury, 1984; Bateman,  
99 1995; Bacon, 1986; Coombs et al., 2000; Troll & Schmicke, 2002; Perugini et al., 2003;  
100 Choe & Jwa, 2004; Janoušek et al., 2004; Prelević et al., 2004; Kumar & Rino, 2006;  
101 Ruprecht et al., 2012; Kim et al., 2014; Weidendorfer et al., 2014). Further complexity arises

102 from uphill diffusion in some species (e.g. Sr, Nd, Al), since diffusion is governed by gradi-  
103 ents in chemical potential rather than concentration, and the temporal dependence of diffusiv-  
104 ities in mixing events caused by changes in temperature and bulk composition (Lesher, 1994;  
105 Bindeman & Davis, 1999).

106

107 Evidence of mixing is preserved primarily at the microscale since the relatively slow rate of  
108 diffusion alone (Morgan et al., 2008; Acosta-Vigil et al., 2012) cannot redistribute chemical  
109 components over large spatial scales (Bindeman & Davis, 1999). Crystals, in particular, can  
110 preserve chemical records of changing storage conditions that can be associated with mixing.  
111 For instance, resorption zones and reverse zoning in plagioclase might indicate changes to  
112 more mafic melt compositions, possibly due to multiple mixing events (Hibbard, 1981;  
113 Tsuchiyama, 1985; Lipman et al., 1997). The mixing history can be determined by combining  
114 these observations with methodologies such as major-element (Rossi et al., 2019), trace-ele-  
115 ment (Humphreys et al., 2009) and isotopic analyses (Davidson et al., 2007), along with  
116 measurements from the bulk rock or other minerals. This can include timescales of mixing  
117 (Chamberlain et al., 2014; Rossi et al., 2019) and ascent (Humphreys et al., 2010), tempera-  
118 tures and pressures of mixing (Samaniego et al., 2011), and the relative contribution of pro-  
119 cesses such as fractional crystallisation (Foley et al., 2012; Ruprecht et al., 2012; Scott et al.,  
120 2013).

121

## 122 *1.2 Physical mingling*

123 Mingling results from fluid flow, either directly due to shear between two magmas during in-  
124 jection, or as a consequence of buoyancy-driven convection. Although mingling cannot occur  
125 in the complete absence of mixing, if convection timescales are shorter than diffusive time-  
126 scales, mingling dominates the interaction and produces heterogeneities that are preserved as  
127 mingling textures if the magma cools and consolidates before homogenisation is complete.  
128 Examples include composite dykes and sills (Wiebe, 1973), intermingled layered intrusions  
129 of alternating composition (Wiebe, 1993; Wiebe, 1998), banded pumice (Clynne, 1999), and  
130 mafic enclaves (Eichelberger, 1980). Enclaves are perhaps the most widely-reported mingling  
131 texture and are widespread in both plutonic (D'Lemos, 1986; 1996; Topley et al., 1990;  
132 Blundy & Sparks, 1992; Williams & Tobisch, 1994; Baxter & Feeley, 2002) and volcanic  
133 (Bacon, 1986; Martin et al., 2006; Browne et al., 2006a,b; Perugini et al., 2007; Fomin &  
134 Plechov, 2012) settings. Enclaves are produced by disaggregation of intrusions into host mag-  
135 mas (Eichelberger, 1980; Thomas, et al., 1993; Tepley et al., 1999; Perugini & Poli, 2005;

136 Hodge, et al., 2012a; 2012b; Caricchi et al., 2012; Andrews & Manga, 2014; Vetere et al.,  
137 2015); Figure 1 illustrates the sizes, shapes and crystallinities that can result. Enclaves often  
138 contain crystals mechanically transferred from the surrounding host magma (xenocrysts),  
139 which can be interrogated to infer conditions (e.g., temperature, crystallinity, melt or bulk  
140 rock composition) at the time of mixing (Reid et al., 1983; Cantagrel et al., 1984; Wiebe,  
141 1993; Coombs et al., 2000; Humphreys et al., 2009; Borisova et al., 2014; Ubide et al., 2014).

142

143 The multi-phase nature of magma is important for mingling dynamics. Experiments have  
144 demonstrated that the presence of phenocrysts can enhance mixing (Kouchi & Sunagawa,  
145 1983; 1985) although a crystal framework can also inhibit efficient mingling (Laumonier et  
146 al., 2014; 2015). Crystallisation-induced degassing (Cashman & Blundy, 2000) of the mafic  
147 end-member due to heat and water loss to the felsic component (Pistone et al., 2017) causes  
148 the exsolution of buoyant volatile phases that can enhance mingling (Eichelberger, 1980;  
149 Wiesmaier et al., 2015). There is also growing recognition that magma storage systems are  
150 dominated by mushy regions with melt concentrated in isolated, possibly transient, lenses  
151 (Hildreth, 1981; 2004; Bachmann & Huber, 2016; Cashman et al., 2017; Sparks et al., 2019).  
152 Despite this, many studies continue to model mingling as taking place between two crystal-  
153 free fluids in a vat (Montagna et al., 2015). Such a picture is hard to reconcile with evidence  
154 from petrological analysis (Turner and Costa, 2007; Druitt et al., 2012; Cooper, 2017) and the  
155 lack of geophysical evidence for large extended bodies of melt (Sinton and Detrick, 1992;  
156 Miller and Smith, 1999; Farrell et al., 2014; Pritchard et al., 2018). It is therefore clear that  
157 the presence of crystals and volatiles, and their effect on magma rheology (Caricchi et al.,  
158 2007; Mueller et al., 2010; Pistone et al., 2012; Mader et al., 2013), must be accounted for  
159 when modelling mingling (Hodge et al., 2012; Andrews & Manga, 2014; Laumonier et al.,  
160 2014).

161

## 162 **2) Controls on magma mingling: Observations, experiments, and numerical models**

163

### 164 *2.1 Field observations*

165 Mingling textures preserved in the field record the varying extents to which magma mingling  
166 can occur. At one extreme, mafic sheets in granite plutons (Bishop & French, 1982; Topley et  
167 al., 1990; Wiebe, 1993, 1998) provide an example of individual intrusions that remain intact  
168 following injection. Multiple injected sheets can create layered intrusions that remain hot for  
169 an extended period of time, although such layers could also result from porosity waves within

170 a mush (Jackson & Cheadle, 1998; Solano et al., 2012). When buoyant (silicic and volatile-  
171 rich) layers underlie mafic sheets, irregular protrusions or pipes of felsic magma are gener-  
172 ated by gravitational instabilities and can penetrate the overlying mafic sheets (Fig. 2; Elwell  
173 et al., 1960; 1962; d’Ars & Davy, 1991; Snyder & Tait, 1995; Caroff et al., 2011). By con-  
174 trast, examples of intimate mingling include compositionally-banded pumice (Clynne, 1999;  
175 Andrews & Manga, 2014), which might have hybridised fully had eruption not interrupted  
176 the mixing process. Enclaves represent an intermediate outcome between layered intrusions  
177 and banded/hybridised products and are the preserved fragments of a disaggregated mafic in-  
178 trusion into a more felsic body. Some, but not all, show fine-grained quenched margins and  
179 coarse, vesicular cores suggesting slower cooling towards the centre of the enclave (Eichel-  
180 berger 1980; Bacon & Metz, 1984; Bacon, 1986; Blundy & Sparks, 1992; Browne et al.,  
181 2006a).

182

183 In mingled rocks, it is common to find crystals derived from one mixing end-member resid-  
184 ing in the other (Fig. 3). Such xenocrysts have been found in composite dykes (Judd, 1893;  
185 King 1964, Prelević et al., 2004; Litvinovsky et al., 2012; Ubide et al. 2014), mafic sheets  
186 (Wiebe, 1993; Wiebe & Collins, 1998; Bishop & French, 1982; Topley et al., 1990) and ba-  
187 saltic lava flows (Iddings, 1890; Diller, 1891; Hiess et al., 2007) but are most commonly de-  
188 scribed in mafic enclaves hosted in both volcanic (Fenner, 1926; Bacon & Metz, 1984; Bacon  
189 1986; Stimac & Pearce, 1992; Coombs et al., 2000; Murphy et al., 2000; Leonard, 2002;  
190 Browne et al., 2006a; Martin et al., 2006; Humphreys et al., 2009; Ruprecht et al., 2012;  
191 Borisova et al., 2014) and plutonic (Reid et al., 1983; D’Lemos, 1986, 1996; Frost & Ma-  
192 hood, 1987; Larsen & Smith, 1990; Pin et al., 1990; Vernon, 1990; Blundy & Sparks, 1992;  
193 Wiebe, 1994; Bateman, 1995; Wiebe et al., 1997; Akal & Helvacı, 1999; Silva et al., 2000;  
194 Baxter & Feeley, 2002; Kim et al., 2002; Choe & Jwa, 2004; Janoušek et al., 2004; Wada et  
195 al., 2004; Kumar & Rino, 2006; Şahin, 2008; Xiong et al., 2012; Kim et al., 2014) rocks.  
196 Textures within these minerals, such as reaction rims on olivine xenocrysts in andesites, can  
197 be used to estimate magma ascent timescales (Reagan et al., 1987; Matthews et al., 1992,  
198 1994; Dirksen et al., 2014; Zhang et al., 2015). Transfer of different minerals can also influ-  
199 ence the mixing signature on Harker diagrams (Ubide et al., 2014). Crystal transfer is likely  
200 to be accompanied by entrainment of its original melt (Cantagrel et al., 1984; Gourgau &  
201 Maury, 1984; Coombs et al., 2000; Wright et al., 2011; Perugini & Poli, 2012; Ubide et al.,  
202 2014). However, direct observation of entrained melt is rare in natural volcanic examples  
203 (Wright et al., 2011) and is not evident in plutons where melts hybridise and crystallise. One

204 example (Fig. 3b) shows an olivine xenocryst in an andesitic lava flow (White Island, New  
205 Zealand), where the crystal is surrounded by a film of basaltic glass (light grey), that is  
206 clearly distinct from the bulk of the lava (dark grey) and is the original melt from which the  
207 olivine crystallised. Such entrainment provides a mechanism by which the crystal's original  
208 magma can 'dilute' the intrusion (Perugini & Poli, 2012; Ubide et al., 2014) and enhance  
209 mingling. However, outstanding questions concerning the role of crystal shape on entrain-  
210 ment remain.

211

212 In addition to xenocryst capture, evidence for crystal transfer from the enclave back to the  
213 host is provided by disequilibrium phenocryst textures indicative of interaction with a more  
214 mafic magma (Cantagrel et al., 1984; Stimac & Pearce, 1992; Clyne, 1999; Nakada & Mo-  
215 tomura, 1999; Tepley et al., 1999; Coombs et al., 2000; Troll & Schmincke, 2002; Ruprecht  
216 & Wörner, 2007; Humphreys et al., 2009; Ruprecht et al., 2012). This can occur through dis-  
217 aggregation of xenocrystic enclaves which disperse their load into the host (Tepley et al.,  
218 1999; Humphreys et al., 2009; Fomin & Plechov, 2012).

219

## 220 *2.2 Analogue experiments*

221 Early analogue experiments used non-magmatic fluids and particles to model magma min-  
222 gling by injecting one viscous fluid into another (Huppert et al., 1984, 1986; Campbell &  
223 Turner, 1986). These studies considered magmas as pure melts and demonstrated that large  
224 viscosity contrasts prohibit efficient mingling. Field observations that some mafic magmas  
225 became vesiculated in response to undercooling by the host magma (Eichelberger, 1980; Ba-  
226 con & Metz, 1984; Bacon, 1986) motivated experiments focussed on bubble transfer from  
227 one viscous layer into another, and demonstrated that the rise of bubble plumes could cause  
228 mingling (Thomas et al., 1993; Phillips & Woods, 2001; 2002). Recent experiments have ex-  
229 amined the effect of crystals on intrusion break-up. For example, Hodge et al. (2012) injected  
230 a particle-rich corn syrup (high density and viscosity) into a large, horizontally sheared body  
231 of particle-free corn syrup (low density and viscosity) to model the injection of cooling (par-  
232 tially crystallised) mafic magma into a convecting magma chamber. They found that low par-  
233 ticle concentrations caused the injection to fragment and form 'enclaves', whereas at high  
234 particle concentrations it remained intact and formed a coherent layer. Although no analogue  
235 experiments have considered liquid injection into variably crystalline suspensions, experi-  
236 ments with gas injection into particle-liquid suspensions show a strong control of particle

237 concentration and injection style, with a threshold between ductile and brittle behaviour at  
238 random close packing (Oppenheimer et al., 2015; Spina et al., 2016).

239

### 240 *2.3. High-temperature and/or high-pressure experiments*

241 Investigations of magma interactions in high-temperature and/or high-pressure experiments  
242 can be broadly divided into two categories. Static experiments consider the juxtaposition of  
243 heated magmas and study mixing resulting from the diffusion of different melt components  
244 (Watson & Jurewicz, 1984; Carroll & Wyllie, 1989; Wylie et al., 1989; Van der Laan &  
245 Wyllie, 1993). Fluid motion can still occur in these static experiments, as variable diffusion  
246 rates between elements can create density gradients that drive compositional convection  
247 (Bindeman & Davis, 1999). Additionally, since water diffuses much more rapidly than other  
248 components (Ni & Zhang, 2008), transfer of water from hydrous mafic magmas to silicic  
249 bodies lowers the liquidus temperature of the latter, leading to undercooling and the produc-  
250 tion of quenched margins in the mafic member, even without a temperature contrast (Pistone  
251 et al., 2016a). Bubbles that exsolve in a lower, mafic layer can also rise buoyantly into the  
252 upper layer, entraining a filament of mafic melt behind them (Wiesmaier et al., 2015). Such  
253 bubble-induced mingling can be highly efficient and has also been documented in natural  
254 samples (Wiesmaier et al., 2015). It has been proposed that a similar style of mingling can  
255 occur through crystal settling (Renggli et al., 2016; Jarvis et al., 2019).

256

257 Dynamic experiments apply shear across the interface between two magmas and reproduce  
258 mingling behaviour. The shear can be applied in various ways, with a rotating parallel plate  
259 geometry (Kouchi & Sunagawa, 1982; 1985, Laumonier et al., 2014; 2015), a Taylor-Couette  
260 configuration (De Campos et al., 2004, 2008; Zimanowski et al., 2004; Perugini et al., 2008),  
261 a Journal Bearing System (De Campos et al., 2011; Perugini et al., 2012) or by using a centri-  
262 fuge (Perugini et al., 2015). These experiments have produced a variety of textures from ho-  
263 mogenous mixed zones to banding. When pure melts are used, the combination of diffusional  
264 fractionation and chaotic advection can produce phenomena such as double-diffusive convec-  
265 tion (De Campos et al., 2008) and reproduce non-linear mixing trends for various major and  
266 trace elements (Perugini et al., 2008; De Campos et al., 2011). Experimental results also sug-  
267 gest new quantities to describe the completeness of mixing, such as the concentration vari-  
268 ance (Perugini et al., 2012) and the Shannon entropy (Perugini et al., 2015). Where crystals  
269 are considered, the presence of phenocrysts can enhance mingling by creating local velocity  
270 gradients and disturbing the melt interface (Kouchi & Sunagawa, 1982; 1985; De Campos et

271 al., 2004). In contrast, other studies (Laumonier et al., 2014; 2015) have shown that the pres-  
272 ence of a crystal framework in the mafic member prevents mingling, whilst the presence of  
273 water can enhance mingling by lowering the liquidus temperature, and thus the crystallinity,  
274 of the magma (Laumonier et al., 2015).

275

#### 276 *2.4 Numerical models*

277 Sparks and Marshall (1986) developed the first simple model to describe viscosity changes  
278 caused by thermal equilibration of a hot mafic magma and a cooler silicic magma, and the re-  
279 sulting (limited) time-window in which mingling/mixing can occur. More sophisticated mod-  
280 els have simulated mingling between melts driven by double-diffusive convection (Olden-  
281 burg, 1989), compositional melting (Kerr, 1994; Cardoso & Woods, 1996) and the Rayleigh-  
282 Taylor instability (Semenov & Polyansky, 2017). Another group of studies has used single-  
283 phase models to simulate elemental diffusion and advection in a chaotic flow field (Perugini  
284 & Poli, 2004; Petrelli et al., 2006). These models reproduce naturally-observed geochemical  
285 mixing relationships, including linear-mixing trends between elements with similar diffusion  
286 coefficients and large degrees of scatter when diffusion coefficients differ (Perugini & Poli,  
287 2004; Nakamura & Kushiro, 1998). Interestingly, the simulations produce both regular and  
288 chaotic regions, which are unmixed and well-mixed, respectively, and have been interpreted  
289 to correspond to enclaves and host rock (Petrelli et al., 2006). This framework has been ex-  
290 tended to account for a solid crystal-phase (Petrelli et al., 2016) by including a Hershel-Buck-  
291 ley shape-dependent rheology (Mader et al., 2013) and a parameterisation of the relationship  
292 between temperature and crystallinity (Nandedekar et al., 2014). This body of work has  
293 demonstrated that chaotic advection can speed-up homogenisation.

294

295 Models of mixing and mingling that consider two-phase magmas containing either solid crys-  
296 tals or exsolved volatiles often assume coupling between the phases. In this way, the solid or  
297 volatile phase can be represented as a continuous scalar field and the resultant effect on rheol-  
298 ogy is accounted for through a constitutive relationship. For example, Thomas and Tait  
299 (1997) used such a framework to show that volatile exsolution in an underplating mafic  
300 magma could create a foam at the interface with an overlying silicic magma. Depending on  
301 the exsolved gas volume fraction and melt viscosity ratio, mixing and mingling could then  
302 proceed through foam destabilisation, enclave formation, or a total overturn of the system.  
303 Folch and Martí (1998) showed analytically that such exsolution could lead to overpressures  
304 capable of causing volcanic eruptions. Recent finite-element models show that injection of a

305 volatile-rich mafic magma into a silicic host can cause intimate mingling when viscosities  
306 and viscosity contrasts are low (Montagna et al., 2015; Morgavi et al., 2019). The combina-  
307 tion of reduced density in the chamber and the compressibility of volatiles can (non-intui-  
308 tively) lead to depressurisation in the chamber (Papale et al., 2017), which is important for  
309 interpretation of ground deformation signals (McCormick Kilbride et al., 2016).

310

311 The effect of crystals on mixing and mingling has also been modelled by treating the crystals  
312 as a continuous scalar field. Examples include simulations of mixing across a vertical inter-  
313 face between a crystal suspension (30% volume fraction) and a lighter, crystal-free magma  
314 (Bergantz, 2000), and injection of a mafic magma into a silicic host with associated melting  
315 and crystallisation (Schubert et al., 2013). The role of crystal frameworks in both the intrud-  
316 ing and host magma is addressed by Andrews and Manga (2014), who model the role of ther-  
317 mal convection in the host, and associated shear stress on the intruding dyke. If convection  
318 occurs whilst the dyke is still ductile, then mingling will produce banding. Otherwise, the  
319 dyke will fracture to form enclaves. Woods and Stock (2019) have also coupled thermody-  
320 namic and fluid modelling to simulate injection, melting and crystallisation in a sill-like ge-  
321 ometry.

322

323 Finally, isothermal computational fluid dynamic simulations have been used to examine the  
324 case of aphyric magma injecting into a basaltic mush. For sufficiently slow injection rates,  
325 the new melt percolates through the porous mush framework, whereas for faster injections,  
326 fault-like surfaces delimit a “mixing bowl” within which the crystals fluidise and energetic  
327 mixing takes place (Bergantz et al., 2015; 2017; McIntire et al., 2019; Schleicher & Bergantz,  
328 2017; Schleicher et al., 2016). By explicitly modelling the particles with a Lagrangian  
329 scheme it is possible to account for particle-scale effects, including lubrication forces (Car-  
330 rara et al., 2019), that are neglected when using constitutive relations from suspension rheol-  
331 ogy. These simulations suggest that mushes with  $\leq 60\%$  crystals can be mobilised by injec-  
332 tion, but neglect welded crystals or recrystallisation of crystal contacts. Furthermore, geo-  
333 physical observations suggest that mushes spend the majority of their lifetimes with much  
334 higher crystallinities (80-90%; Sinton and Detrick, 1992; Farrell et al., 2014; Pritchard et al.,  
335 2018).

336

337 **3) Petrologic constraints on mingling conditions: Petrographic interpretations**

338 Here, through the use of examples, we show how the texture and chemistry of enclaves and  
339 xenocrysts have been interrogated to interpret information on mixing and mingling processes.  
340 Although many studies have examined mixed and mingled rocks from both plutonic and vol-  
341 canic realms, here we review work on examples from four volcanoes (Chaos Crags and Las-  
342 sen Peak, both USA; Mt. Unzen, Japan; and Soufrière Hills, Montserrat) which have erupted  
343 intermediate composition lavas containing mafic enclaves (Fig. 4). We use common features,  
344 as recorded in the literature and augmented by an additional sample of Mt. Unzen lava from  
345 the 1792 dome collapse deposit, to develop a conceptual model that describes how volatile  
346 and crystals contents control mixing and mingling in magma storage regions. We analyse the  
347 latter using back-scatter electron images (BSE) obtained using both a Hitachi S-3500N (Uni-  
348 versity of Bristol) and a Tescan Mira II (University of Lausanne) scanning electron micro-  
349 scope (SEM). Plagioclase compositions were measured on a Cameca SX100 (University of  
350 Bristol) with an accelerating voltage of 20 kV, emission current of 10 nA and a spot size of 3  
351  $\mu\text{m}$ .

352

### 353 *3.1. Volcanic systems*

354

#### 355 *3.1.1 Chaos Crags*

356 Chaos Crags comprises of a series of enclave-bearing rhyodacite lava domes that erupted be-  
357 tween 1125 and 1060 years ago (Clynne, 1990). The host lavas are crystal-rich, containing  
358 phenocrysts of plagioclase, hornblende, biotite and quartz, whilst the enclaves are basaltic an-  
359 desite to andesite with occasional olivine, clinopyroxene and plagioclase phenocrysts in a  
360 groundmass of amphibole and plagioclase microphenocrysts (Heiken & Eichelberger, 1980).  
361 Many, but not all, enclaves have fine-grained and crenulated margins and all contain resorbed  
362 phenocrysts captured from the host (Fig. 4a). Some phenocrysts in the host also show resorp-  
363 tion textures (Tepley et al., 1999).

364

#### 365 *3.1.2 Lassen Peak*

366 Lassen Peak erupted in 1915, producing a dacite dome and lava flow followed by a sub-Pli-  
367 nian eruption that deposited two types of pumice: homogeneous dacite and banded dacite/an-  
368 desite. The dome and flow are porphyritic with phenocrysts of plagioclase, biotite, horn-  
369 blende and quartz in a glassy, vesicular groundmass containing microphenocrysts of plagio-  
370 clase, pyroxenes and Fe-Ti oxides. The dacite dome and lava flow also contain xenocryst-  
371 bearing andesitic enclaves with equigranular texture and a lack of crenulated margins (Fig.

372 4b; Clynne, 1999). The enclaves have olivine phenocrysts (which occasionally appear as xen-  
373 ocrysts in the host) with plagioclase and pyroxene microphenocrysts.

374

### 375 *3.1.3 Mt. Unzen*

376 Mt. Unzen has erupted lavas and domes since 300-200 ka (Hoshizumi et al., 1999), most re-  
377 cently during the 1991-1995 eruption. With the exception of an andesitic lava flow from  
378 1663, Mt. Unzen lavas are consistently dacitic, containing basaltic to andesitic enclaves  
379 (Hoshizumi et al., 1999; Browne et al., 2006a). Dacite erupted in the 1991-1995 eruption is  
380 porphyritic with about 20% phenocrysts of plagioclase, hornblende, biotite and quartz, with  
381 plagioclase, pargasite, pyroxenes, apatite and Fe-Ti oxides occurring as microlites in a highly  
382 crystalline groundmass (Nakada & Fuji, 1993; Nakada et al., 1999; Nakada & Motomura,  
383 1999; Venezky & Rutherford, 1999; Cordonnier et al., 2009; Hornby et al., 2015). Two types  
384 of enclaves are observed: porphyritic and equigranular. Porphyritic enclaves contain large  
385 crystals of plagioclase, hornblende and rare quartz within a finer groundmass of plagioclase  
386 and hornblende microphenocrysts, minor amounts of clinopyroxene and olivine, and intersti-  
387 tial glass (Fig. 4c). The overall crystallinity is 70-90%. Equigranular enclaves contain equant  
388 microphenocrysts of plagioclase with smaller quantities of hornblende and orthopyroxene  
389 (Browne et al., 2006a).

390

### 391 *3.1.4 Soufrière Hills*

392 The 1995-2010 Soufrière Hills eruption produced a series of andesitic lava domes containing  
393 enclaves of basaltic to basaltic-andesitic composition (Wadge et al., 2014; Plail et al., 2014).  
394 The andesite contains approximately 40% phenocrysts (plagioclase, hornblende, orthopyrox-  
395 ene, Fe-Ti oxides and minor quartz) in a much finer-grained groundmass with up to 25%  
396 glass (Murphy et al. 2000; Humphreys et al., 2009; Edmonds et al., 2016). The enclaves have  
397 a diktytaxitic groundmass of plagioclase, pyroxenes, amphibole and Fe-Ti oxides with larger  
398 xenocrysts inherited from the andesite (Fig. 4d). Some enclaves have crenulated and fine-  
399 grained margins, whereas others are more equigranular and of a less mafic composition (Mur-  
400 phy et al., 2000; Plail et al., 2014; 2018).

401

## 402 *3.2 Phenocryst, xenocryst and groundmass textures and chemistries*

403

### 404 *3.2.1 Enclave groundmass textures*

405 The enclaves from all four volcanoes show both similar and contrasting textural features. At  
406 Chaos Crags, most enclaves have fine-grained and crenulate margins (Fig. 4a; Tepley et al.,  
407 1999), although those erupted in later domes are more angular and lack fine-grained margins.  
408 Enclaves in Lassen Peak samples are subrounded to subangular with an equigranular texture  
409 (Fig. 4b; Clynne, 1999). Many enclaves from the 1991-1995 eruption at Mt. Unzen have  
410 crenulate and fine-grained margins (Browne et al., 2006), although some have angular edges  
411 and a uniform crystal size (Fig. 4c; Fomin & Plechov, 2012). Similar features are observed at  
412 Soufrière Hills, with many inclusions being ellipsoidal (Fig. 4d) and some angular; most, but  
413 not all, have fine-grained, crenulate margins (Murphy et al., 2000). Both the size and volume  
414 fraction of enclaves increased during the eruption (Barclay et al., 2010; Plail et al., 2014;  
415 2018).

416

417 In all localities, fine-grained margins and crenulate contacts are attributed to undercooling of  
418 the mafic magma due to juxtaposition against the much cooler felsic host (Eichelberger,  
419 1980) and associated rapid crystallisation of the mafic melt near the contact with the felsic  
420 host. These crystalline rims have a greater rigidity than the lower-crystallinity enclave interi-  
421 ors so that as the enclave continues to cool and contract, the rims deform to a crenulate shape  
422 that preserves the original surface area (Blundy & Sparks, 1992). Enclaves not exhibiting  
423 such quench textures are also found at all localities.

424

### 425 3.2.2 Plagioclase

426 The composition and texture of plagioclase crystals are extremely good recorders of mag-  
427 matic processes because 1) their stability field in pressure-temperature-composition (P-T-X)  
428 space is very large in volcanic systems, and 2) compositional zoning modulated by changes  
429 in the P-T-X space is well preserved due to the relatively slow diffusion in the coupled substi-  
430 tution between Na-Si and Ca-Al (Grove et al., 1984; Morse, 1984; Berlo et al., 2007).

431

432 Texturally, plagioclase phenocrysts in the host lavas at all four localities comprise a popula-  
433 tion of unreacted, oscillatory zoned crystals with a lesser amount of reacted crystals that have  
434 sieved cores and/or resorption rims (Fig 5a; Tepley et al., 1999; Clynne 1999; Murphy et al.,  
435 2000; Browne et al., 2006b). Associated enclaves contain plagioclase xenocrysts incorporated  
436 from the host with sieved-texture resorption zones that consist of patchy anorthite-rich plagi-  
437 oclase and inclusions of glass (quenched melt). These reacted zones can penetrate to the cores

438 of smaller crystals (Fig. 5b,c), but in larger xenocrysts appear as a resorption mantle sur-  
439 rounding a preserved oscillatory-zoned core (Fig. 5d). All xenocrysts are surrounded by a  
440 clean rim that is of the same composition as the plagioclase microphenocrysts in the enclave  
441 groundmass.

442

443 The relationship between anorthite (An) and FeO content of plagioclase crystals can also pro-  
444 vide insight into magma mixing and mingling. Plagioclase crystals erupted from Soufrière  
445 Hills volcano between 2001 and 2007 show a shallow, linear trend between FeO and An con-  
446 tents in oscillatory-zoned regions of plagioclase phenocrysts in the host (Humphreys et al.,  
447 2009); sieved zones in the same phenocrysts form a curved trend at higher FeO (Fig. 6d). In  
448 enclave-hosted xenocrysts, oscillatory-zoned cores plot on the same linear trend as oscilla-  
449 tory-zoned phenocrysts, whereas the clean rims overlap with the curved trend of the pheno-  
450 cryst sieved zones (Fig. 6f). The same curved trend is found for enclave microphenocrysts  
451 (Fig. 6e; Humphreys et al., 2009). We observe similar characteristics in our sample of Mt. Un-  
452 zen dome lava (Figs. 6a-c).

453

### 454 3.2.3 Quartz

455 Quartz crystals in mingled lavas can also show distinctive features. Host phenocrysts are  
456 rounded and embayed (Fig. 7a; Clyne, 1999; Tepley et al., 1999; Murphy et al., 2000;  
457 Browne et al., 2006a; Christopher et al., 2014) and can also be fractured (Clyne, 1999). In  
458 the enclaves, quartz xenocrysts are surrounded by reaction rims of clinopyroxene and horn-  
459 blende microphenocrysts and glass (Fig 7b; Clyne, 1999; Tepley et al., 1999; Murphy et al.,  
460 2000; Browne et al., 2006).

461

### 462 3.3 Interpretation of textures and chemistries

463 The common textural and chemical features of these volcanic systems suggest commonalities  
464 in the mixing and mingling processes. First, since enclaves from all volcanoes contain xeno-  
465 crysts that originated in the host magmas, the mafic component must have been sufficiently  
466 ductile to incorporate these crystals during mixing. Plagioclase xenocrysts contain rounded,  
467 patchy zones with a sieved texture showing that both partial and simple dissolution occurred  
468 (Tsuchiyama, 1985; Nakamura & Shimakita, 1998; Cashman & Blundy, 2013), suggesting  
469 that the enclave magmas were undersaturated in plagioclase at the time of incorporation.  
470 Since up to 70% of the enclave groundmass consists of plagioclase microphenocrysts, this  
471 implies the mafic magmas were crystal-poor at the time of xenocryst incorporation.

472

473 Compositional variations of FeO and An in the plagioclase crystals provide further infor-  
474 mation on the relative compositions of the host and enclave melt at Soufrière Hills (Hum-  
475 phreys et al., 2009) and Mt. Unzen (Fig. 6). Most analyses from host phenocrysts show a  
476 shallow, increasing linear trend between An and FeO content (Fig. 6a,d); the few points with  
477 FeO enrichment correspond to resorbed zones. Unresorbed cores of xenocrysts have similar  
478 compositions, suggesting that both crystal core populations derive from the same host dacite  
479 magma. Enclave microphenocrysts, however, show greater FeO enrichment (Figs. 6b,e) and  
480 overlap with xenocrysts rim compositions. Similar results are reported for plagioclase in an-  
481 desite lavas erupted from El Misti, Peru, which underwent resorption in response to mafic re-  
482 charge (Ruprecht & Wörner, 2007). At Mt. Unzen, enclave microphenocrysts and xenocrysts  
483 rims show a strong positive correlation for the whole An range, whilst these phases at Sou-  
484 frière Hills show a negative correlation for An > 75 mol% (Fig. 6). This difference is inter-  
485 preted to reflect the absence of Fe-Ti oxide as an early crystallising phase in the Soufrière  
486 Hills mafic end-member, which would cause FeO to increase in the residual melt as other  
487 phases precipitated until the point of oxide saturation (Humphreys et al., 2009). The lack of  
488 this inflection in the Mt. Unzen sample suggests that Fe-Ti oxides were present in the mafic  
489 magma prior to mixing, as suggested for the 1991-1995 eruption (Holtz et al., 2005; Botchar-  
490 nikov et al., 2008).

491

492 Whereas the observed enrichment in FeO in enclave microphenocrysts, sieved zones in phe-  
493 nocrysts and xenocrysts, and xenocrysts rims is likely due to crystallisation from a more  
494 mafic melt, it is also possible that growth of these regions may be sufficiently fast for kinetic  
495 effects to play a role; if growth is faster than diffusion of FeO in the melt then an FeO-rich  
496 boundary layer may develop around crystals (Bottinga et al., 1966; Bacon, 1989; Mollo et al.,  
497 2011) that could also explain the enrichment. However, such a process would generate a neg-  
498 ative correlation between FeO and An (Neill et al., 2015), not the positive correlation ob-  
499 served at Unzen and Soufrière Hills.

500

501 The contrasting textures of quartz in the host and enclaves also provide insight into the min-  
502 gling/mixing process. Rounding of quartz xenocrysts, together with glass-filled embayments,  
503 suggests dissolution of quartz in the host. Conversely, quartz reaction rims comprising horn-  
504 blende microphenocrysts, glass and vesicles in the enclaves (Figures 3d, 7b) suggest that the

505 dissolution-induced increase in the silica content (and H<sub>2</sub>O solubility) of the surrounding melt  
506 caused diffusion of H<sub>2</sub>O towards the quartz (Pistone et al., 2016a).

507

508 Whereas the presence of resorbed xenocrysts in enclaves suggests that there was time for  
509 crystals to be incorporated, and to react, before the enclave started to crystallise, the presence  
510 of fine-grained rims on some enclaves (Tepley et al., 1999; Murphy et al., 2000; Browne et  
511 al., 2006a; Barclay et al., 2010; Plail et al., 2014) implies rapid cooling and crystallisation  
512 (chilling) of the mafic magma against the cooler silicic host (Bacon, 1986). Xenocrysts must  
513 therefore have been incorporated prior to the formation of the chilled margin, providing a  
514 limited temporal window for crystal transfer. A comparison of the thickness of xenocryst re-  
515 sorption zones at Mt. Unzen (Brown et al. 2006a) with those produced experimentally  
516 (Tsuchiyama & Takahasi, 1983; Tsuchiyama, 1985; Nakamura & Shimakita, 1998) suggests  
517 resorption on a timescale of days; this contrasts with thermal modelling (Carslaw & Jaeger,  
518 1959) suggesting enclaves should thermally equilibrate on a timescale of hours. Again, this  
519 requires incorporation of xenocrysts prior to intrusion disaggregation and enclave formation  
520 (Browne et al., 2006a). As the considered volcanic lavas contain similarly resorbed plagio-  
521 clase xenocrysts within enclaves of comparable sizes, it seems likely that this temporal con-  
522 straint on the sequence of crystal transfer prior to enclave formation is generally true for the  
523 systems presented here.

524

525 Importantly, all locations also contain enclaves with unquenched margins (Tepley et al.,  
526 1999; Plail et al., 2014) and equigranular textures (Heiken & Eichelberger, 1980; Browne et  
527 al., 2006a). Equigranular enclaves at Mt. Unzen have been interpreted as originating from  
528 disaggregation of the interior of the intruding magma, which cooled more slowly than the in-  
529 trusion margin where porphyritic enclaves (xenocrysts-bearing, chilled margin) formed. Sim-  
530 ilarly, at Soufrière Hills, the quenched enclaves may form from an injected plume of mafic  
531 magma, whereas unquenched and more hybridised enclaves form from disturbance of a hy-  
532 brid layer at the felsic-mafic interface (Plail et al., 2014). Angular enclaves with unquenched  
533 margins may record the break-up of larger enclaves (Clynne, 1999; Murphy et al, 2000;  
534 Fomin & Plechov, 2012; Plail et al., 2014), which can return resorbed host-derived crystals to  
535 the host; this explains the presence of resorption zones in crystals in the host lavas (Fig. 5b),  
536 and chemical signatures (Fig. 6a) of crystallisation from mafic magma. Further support for  
537 enclave fragmentation comes from microlites that are chemically indistinguishable from en-  
538clave phases at Soufrière Hills (Humphreys et al., 2009). A possible method to determine

539 whether equigranular enclaves form from a hybrid layer or disaggregation of larger enclaves  
540 is to examine the mineralogy of the crystals in the enclave. The two different mechanisms  
541 will produce different degrees of undercooling within the enclave magma, which, in the hy-  
542 brid-layer model, will depend on the relative proportions of the end-member magmas, and  
543 thus can produce different crystal assemblages/textures (Humphreys et al., 2006).

544

#### 545 *3.4. Conceptual model of magma mixing and mingling*

546 Common features of eruptive products described above suggest common aspects of mixing  
547 and mingling. Xenocrystic mafic enclaves with chilled margins, in particular, require that  
548 magma injection is accompanied by crystal incorporation from the host magma, as also sug-  
549 gested by a comparison of thermal timescales with the times needed to generate the observed  
550 thicknesses of resorption zones (Browne et al., 2006a). These constraints on the sequence of  
551 mixing processes have led to a similar conceptual model of mixing and mingling (Fig. 8;  
552 Clynne, 1999; Tepley et al., 1999; Murphy et al., 2000; Browne et al., 2006; Plail et al., 2014)  
553 in which the mafic magma is injected as a fountain (Clynne, 1999) or collapsing plume (Plail  
554 et al., 2014) before ponding at the base of the silicic host (Fig. 8a). Shear caused by the injec-  
555 tion disrupts the interface between the two magmas, leading to the formation of blobs of hy-  
556 bridised magma with incorporated host crystals that then rapidly chill against the silicic host,  
557 preventing further hybridisation (Tepley et al., 1999; Plail et al., 2014). Heating of the host, in  
558 turn, causes partial melting, reducing the crystallinity and causing convective motions that  
559 disperse the enclaves. Meanwhile, at the mafic-silicic contact, a hybrid interface layer forms  
560 (Fig. 8b). As this layer crystallises, second boiling drives fluid saturation; exsolved buoyant  
561 fluids produce a low-density, gravitationally-unstable, interface layer that breaks-up to form  
562 further enclaves (Fig. 8c; Clynne, 1999; Browne et al., 2006a). As cooling propagates down-  
563 wards through the mafic body, enclaves can come from deeper portions resulting in more  
564 equigranular enclaves that lack chilled margins or xenocrysts (Brown et al., 2006a; Plail at  
565 al., 2014).

566

567 Enclaves, once formed, can disaggregate. Disaggregation is shown by the presence of broken  
568 enclaves (Clynne, 1999; Tepley et al., 1999; Fomin & Plechov, 2012), host phenocrysts with  
569 resorption zones and Fe enrichment caused by previous engulfment in mafic magma (Clynne,  
570 1999; Tepley et al., 1999; Browne et al., 2006b; Humphreys et al., 2009), and small clusters  
571 of enclave-derived microlite material within the host lavas (Humphreys at al., 2009). Dis-

572 aggregation allows for subsequent mixing of a type precluded during initial enclave for-  
573 mation, but the timing of disaggregation is poorly constrained. It could occur during high-  
574 shear conditions in the conduit (Humphreys et al., 2009); alternatively, disaggregation may  
575 be part of a continuous cycle of injection, enclave formation and fragmentation (Fig. 8d) that  
576 gives rise to a continuously convecting magma storage region, which is sometimes sampled  
577 during a volcanic eruption (Browne et al., 2006a). Regardless, the dispersion of mafic  
578 groundmass into the host has implications for interpreting end-member compositions from  
579 petrologic studies (Martel et al., 2006; Humphreys et al., 2009). Importantly, neglecting such  
580 transfer can lead to an under-estimate of the initial silica content of the felsic member.

581

#### 582 **4 Quantitative modelling of crystal and volatile controls on mixing and mingling**

583

584 Many conceptual models of magma mixing (e.g. Fig. 8) have been produced based on petro-  
585 logic evidence. However, quantitative models of magma mixing are limited. As described in  
586 Section 2.3, Sparks and Marshall (1986) first developed a simple model describing how ther-  
587 mal equilibration of a juxtaposed mafic and silicic magma led to rapid viscosity changes that  
588 inhibited mixing after a short time. Since then, models developed to account for the role of  
589 either crystals or exsolved volatiles have produced significant insights into mingling and mix-  
590 ing dynamics, but have failed to incorporate petrological data within quantitative frame-  
591 works. Here, we examine three models: Andrews and Manga (2014), who use continuum  
592 modelling and suspension rheology to model mingling resulting from dyke injection into a  
593 silicic host; Bergantz et al. (2015), who model the injection of melt into a basaltic mush, re-  
594 solving both fluid and granular behaviour; and Montagna et al. (2015), who simulate the ef-  
595 fect of exsolved volatiles on mafic injection. We compare the model assumptions and results,  
596 as well as their implications for interpreting petrological data.

597

##### 598 *4.1 The model of Andrews and Manga (2014)*

599 The model considers the instantaneous injection of a mafic dyke into a silicic host, with a  
600 prescribed initial composition and temperature, and numerically solves the 1D heat equation.  
601 Changes in the crystallinity and bulk viscosity of magmas with time are calculated using  
602 MELTS simulations (Ghiorso & Sack, 1995; Asimow & Ghiorso, 1998) and viscosity models  
603 for melt (Giordano et al., 2008) and crystal-bearing suspensions (Einstein, 1906; Roscoe,  
604 1952). If the viscosity of the host immediately juxtaposed with the dyke decreases suffi-  
605 ciently, then the host starts to convect (as determined by a Rayleigh number criterion), which

606 exerts a shear stress on the dyke. If this shear stress exceeds the yield stress of the dyke  
607 (which depends on its crystal content), the dyke deforms in a ductile fashion and the model  
608 predicts banded products. Alternatively, if the yield stress exceeds the shear stress, then the  
609 dyke fractures in a brittle fashion and enclaves form.

610

611 In this model context the principal control on mingling dynamics is the development of crys-  
612 tal frameworks within the dyke. Dyke crystallisation, in turn, is controlled by composition  
613 and temperature contrasts. For example, injection of hot, large and wet dykes causes the si-  
614 licic host to convect before a crystal framework forms in the dyke. The resultant shear causes  
615 ductile disruption of the dyke and intimate mingling of the two magmas, producing banding  
616 and, with time, homogenisation. Small and dry dykes, in contrast, experience extensive crys-  
617 tallisation before the host starts to convect and thus fracture to form enclaves. The precise ini-  
618 tial conditions (temperature, dyke size and water content) that determine mingling style are  
619 sensitive to the parameterisations used (e.g. critical Rayleigh number for convection) but the  
620 qualitative results are useful.

621

622 The principal limitation of the model of Andrews and Manga (2014) is that it assumes an in-  
623 stantaneous injection of the mafic dyke and therefore neglects any mixing/mingling that oc-  
624 curs during injection itself. Instead, the dyke is disrupted only by shear due to convection in  
625 the host. Indeed, the relative importance of shear due to injection versus shear due to convec-  
626 tion remains a considerable unknown. The assumption that brittle fragmentation of the dyke  
627 produces enclaves is supported by three-dimensional tomographic observations of enclaves  
628 from Chaos Crags, which have crystal frameworks that are lacking in banded pumices from  
629 Lassen Peak (Andrews & Manga, 2014). The inference is that these crystal frameworks cre-  
630 ated a yield stress such that the enclaves formed by solid-like fracturing and banded pumice  
631 by ductile deformation. However, this is in direct contradiction with the conceptual model  
632 presented above (Fig. 8), which is based on field and petrographic observations that suggest  
633 enclaves form from fluid-like deformation of the mafic magma. This contradiction highlights  
634 the extent to which conditions of enclave formation are unknown.

635

#### 636 *4.2 The model of Bergantz et al., (2015)*

637 The discrete-element model, which resolves both fluid and granular physics, considers the in-  
638 jection of a crystal-free magma into the base of a crystal mush at random loose packing (ap-  
639 proximately 60% crystallinity). The response of the mush is governed by stress chains formed

640 by crystal-crystal contacts. For sufficiently slow injections, the new melt permeates through  
641 the mush, which behaves as a porous medium. Once the injection speed is large enough to  
642 disrupt the stress chains, however, part of the mush can become fluidised to form a mixing  
643 cavity, which is an isolated region where the host melt, crystals and new melt undergo over-  
644 turning. The new melt then escapes from the cavity through porous flow into the rest of the  
645 mush. For still faster flow speeds, the stress chains orientate to create two fault-like surfaces  
646 at angles of about  $60^\circ$  to the horizontal that bound a fluidised region of the mush, within  
647 which extensive circulation occurs.

648

649 Whilst this model captures granular and fluid dynamics on the crystal scale and demonstrates  
650 the impact of varying the injection velocity, there are numerous outstanding questions.

651 Firstly, varying the crystallinity of the mush has not been addressed and will presumably af-  
652 fect the values of injection velocity at which transitions between mingling styles occur. Fur-  
653 thermore, temporal and spatial variations in temperature (due to heat transfer or latent heat  
654 release), and therefore in viscosity and crystallinity, have not been considered. Cooling and  
655 crystallisation of the new melt should control the dynamics of the system, as will associated  
656 latent heat release. Finally, the geometry of the modelled magma reservoir (laterally homoge-  
657 nous layers) will affect the specifics of the mixing process, such as the orientation of the  
658 bounding faults, and it is not yet clear if the model scales to natural systems.

659

#### 660 *4.3. The model of Montagna et al. (2015)*

661 The two-dimensional finite-element model considers two vertically-separated magma cham-  
662 bers that are superliquidus and connected by a narrow conduit. The upper chamber initially  
663 contains a felsic phonolite, whilst the lower chamber and conduit are filled with a mafic sho-  
664 shonite, compositions chosen to represent eruptions from Campi Flegrei.  $H_2O$  and  $CO_2$   
665 exsolve as functions of temperature and pressure (Papale et al., 2006), whilst the transport of  
666 exsolved volatiles is modelled as a continuum scalar field satisfying a transport equation.

667 Bubbles are assumed to be sufficiently small that they are undeformable and an empirical law  
668 is used to parameterise their effect on bulk viscosity (Ishii & Zuber, 1979). The shoshonite  
669 initially contains exsolved volatiles and so is lighter than the phonolite, creating an unstable  
670 density interface at the inlet to the upper chamber.

671

672 Upon initiation, a Rayleigh-Taylor instability develops at the inlet to the upper chamber and a  
673 plume of light material rises into the chamber whilst the conduit is filled with a mixed, hybrid

674 magma. Intimate mingling within the chamber is reminiscent of that created by chaotic ad-  
675 vection (Perugini & Poli, 2004). The magma entering the upper chamber is a partial hybrid,  
676 and the pure parent shoshonite never enters the upper conduit. Intensive mingling occurs on a  
677 timescale of hours, promoted by a large initial density contrast and horizontally-elongated  
678 chambers. Importantly, the reduction in density of the upper chamber can cause depressurisa-  
679 tion, which has implications for interpreting ground deformation signals (Papale et al., 2017).

680

681 Whilst an obvious limitation of the model is the two-dimensional domain, it seems reasonable  
682 that the results can be extrapolated to three-dimensional systems. A greater limitation is the  
683 restricted range of compositions and temperatures for which the model is valid. The end-  
684 member compositions are similar and superliquidus, so that both the absolute bulk viscosities  
685 ( $< 3500 \text{ Pa s}$ ) and their contrast (factor of 7) are relatively low. This allows rapid mingling  
686 and ignores entirely the effect of crystals on the flow dynamics.

687

#### 688 *4.4. Comparison and common limitations*

689 Both Andrews and Manga (2014) and Bergantz et al. (2015) focused on the effect of crystals,  
690 but a key difference in the two models is the initial condition. Andrews and Manga (2014) as-  
691 sume the instantaneous injection of a dyke into an initial rheologically-locked host, whereas  
692 Bergantz et al. (2015) simulate the flow of new melt into a melt-crystal mixture; they show  
693 that new melt flows permeably through a rheologically-locked mush. The conditions that spa-  
694 tially constrain a mafic injection (e.g. as a dyke) have not been defined. The two models also  
695 simulate the role of crystals differently. Andrews and Manga (2014) calculate the crystallinity  
696 of a magma at a given temperature and assume the presence of a crystal framework (and yield  
697 stress) above a threshold value. Bergantz et al. (2015) allow the crystals to form force chains  
698 through which stresses are transmitted (Bergantz et al., 2017), but they consider the system to  
699 be isothermal such that no crystallisation occurs, a key feature of Andrews and Manga  
700 (2014).

701

702 Both models are limited in addressing the role of volatiles. Diffusion of volatiles from the  
703 mafic to felsic member can strongly influence the crystal composition and textures of the si-  
704 licic member (Pistone et al., 2016a), while exsolution of volatiles leads to a reduction in bulk  
705 density that can drive convective motions in the mixing dynamics (Eichelberger, 1980;  
706 Thomas et al., 1993; Phillips & Woods, 2001; 2002; Montagna et al., 2015; Wiesmaier et al.,  
707 2015). The presence of exsolved volatiles also affects the magma rheology and requires the

708 use of three-phase rheological models (Mader et al., 2013; Pistone et al., 2016b). One strat-  
709 egy is to treat the exsolved phase as a continuum scalar field and use a suspension model for  
710 bulk rheology (Montagna et al., 2015). However, as has been shown for solid phases (Carrara  
711 et al., 2019), small scale effects can be overlooked by this approach and explicit modelling of  
712 such phases may be needed to accurately constrain mixing/mingling processes.

713

714 Additional complications arise in the number of parameters required for a given model. For  
715 example, the Andrews and Manga (2014) model requires values for a maximum crystal pack-  
716 ing fraction and a critical Rayleigh number for convection in the host. Constraining these pa-  
717 rameters will require extensive experimental efforts involving both high-temperature/high-  
718 pressure and analogue experiments.

719

## 720 **5. Conclusions and outlooks for future research**

721 We have reviewed progress in understanding magma mixing and mingling, focusing on vola-  
722 tile and crystal controls on mingling processes. Whilst field and petrologic observations of  
723 mixed and mingled products are numerous, models of these processes do not yet include the  
724 full range of observed complexities. In particular, conceptual models derived from observa-  
725 tions (Clynne, 1999; Tepley et al., 1999; Browne et al., 2006; Plail et al., 2014) suggest very  
726 different dynamics to those from numerical models (Andrews & Manga, 2014; Bergantz et  
727 al., 2015; Montagna et al., 2015). To resolve this discrepancy, several key questions need to  
728 be addressed:

- 729 1) How do mixing and mingling occur within the framework of crystal mushes, and how  
730 does the volume fraction of crystals control the interaction dynamics?
- 731 2) How do volatiles, both exsolved and dissolved, affect mixing and mingling? What is the  
732 relative importance of chemical quenching (due to volatile diffusion) vs. thermal  
733 quenching (due to heat diffusion)?
- 734 3) How much mingling/mixing takes place during intrusion of the mafic magma compared  
735 to that driven by later processes such as convection in the host or the buoyant rise of  
736 vesicular mafic/hybrid magma?
- 737 4) How does latent heat, released from crystallisation of the mafic component and absorbed  
738 by melting of the felsic component, affect the mixing and mingling process? Latent heat

739 release may have a strong local effect in a dynamic system but is not evaluated, for  
740 example, in isothermal experiments.

741 5) To what extent are mafic injections spatially limited, e.g. dykes, and under what  
742 conditions might they affect the entire intrusion?

743 6) If magma storage regions undergo repeated replenishments with occasional eruptions,  
744 what factors determine if a particular injection leads to an eruption?

745 Only by combining field and analytical observations with experimental (analogue and natural  
746 materials) and numerical modelling can we start to address these challenges.

747

#### 748 Acknowledgements

749 PAJ was supported by the National Environmental Research Council (grant number  
750 NE/K500823/1) and thanks Alison Rust, Steve Tait and Julie Oppenheimer for valuable dis-  
751 cussions. The authors acknowledge Stuart Kearns, Ben Buse (University of Bristol), Pierre  
752 Vonlanthen and Martin Robyr (University of Lausanne) for their support during SEM and  
753 EPMA analyses. MP acknowledges funds from the Ambizione Fellowship (PZ00P2\_168166)  
754 sponsored by the Swiss National Science Foundation, which supported the batchelor's thesis  
755 of AS. KVC acknowledges funding from the AXA Research Fund and a Wolfson Merit  
756 Award from the Royal Society.

757

#### 758 References

759 Acosta-Vigil A, London D & Morgan VI, G. B. (2012). Chemical diffusion of major compo-  
760 nents in granitic liquids: implications for the rates of homogenization of crustal melts. *Lithos*  
761 *153*, 308–323. <https://doi.org/10.1016/j.lithos.2012.06.017>

762

763 Adkins, P. (1983). *Equilibrium Thermodynamics*. Cambridge: Cambridge University Press.

764

765 Andrews, B. J. & Manga, M. (2014). Thermal and rheological controls on the formation of  
766 mafic enclaves or banded pumice. *Contrib. Mineral. Petrol.*, *167*, 961.

767 <https://doi.org/10.1007/s00410-013-0961-7>

768

769 Akal, C. & Helvacı, C. (1999). Mafic Microgranular Enclaves in the Kozak Granodiorite,  
770 Western Anatolia. *Turkish J. Earth Sci.* *8*, 1-17.

771

772 Arzi, A. A. (1978). Critical phenomena in the rheology of partially melted rocks. *Tectono-*  
773 *physics*, *44*, 73-184.

774

775 Bachmann, O. & Huber, C. (2016). Silicic Magma reservoirs in the Earth's Crust. *Am. Min-*  
776 *eral.*, *101*, 2377-2404. <http://dx.doi.org/10.2138/am-2016-5675>

777

778 Bacon, C. (1986). Magmatic Inclusions in Silicic and Intermediate Volcanic Rocks. *J. Geophys. Res.*, *91(B6)*, 6091-6112. <https://doi.org/10.1029/JB091iB06p06091>  
779  
780  
781 Bacon, C. R. (1989). Crystallization of accessory phases in magmas by local saturation adjacent to phenocrysts. *Geochim. Cosmochim. Acta.*, *53(5)*, 1055-1066.  
782  
783 [https://doi.org/10.1016/0016-7037\(89\)90210-X](https://doi.org/10.1016/0016-7037(89)90210-X)  
784  
785 Bacon, C. R. & Metz, J. (1984). Magmatic inclusions in rhyolites, contaminated basalts, and  
786 compositional zonation beneath the Coso volcanic field. *Contrib. Mineral. Petrol.*, *85*, 346-  
787 365. <https://doi.org/10.1007/BF01150292>  
788  
789 Barclay, J., Herd, R. A., Edwards, B. R., Christopher, T., Kiddle, E. J., Plail, M. & Donovan,  
790 A. (2010). Caught in the act: Implications for the increasing abundance of mafic enclaves  
791 during the recent eruptive episodes of the Soufrière Hills Volcano, Montserrat. *Geophys. Res. Lett.*, *37*, L00E09. <https://doi.org/10.1029/2010GL042509>  
792  
793  
794 Bateman, R. (1995). The interplay between crystallisation, replenishment and hybridization  
795 in large felsic magma chambers. *Earth-Sci. Rev.*, *39(1-2)*, 91-106.  
796 [https://doi.org/10.1016/0012-8252\(95\)00003-S](https://doi.org/10.1016/0012-8252(95)00003-S)  
797  
798 Baxter, S. & Feely, M. (2002). Magma mixing and mingling textures in granitoids: examples  
799 from the Galway Granite, Connemara, Ireland. *Mineral. Petrol.*, *76(1-2)*, 63-74.  
800 <https://doi.org/10.1007/s007100200032>  
801  
802 Bergantz, G. W. (2000). On the dynamics of magma mixing by reintrusion: implications for  
803 pluton assembly processes. *J. Struct. Geol.*, *22*, 1297-1309. [https://doi.org/10.1016/S0191-](https://doi.org/10.1016/S0191-8141(00)00053-5)  
804 [8141\(00\)00053-5](https://doi.org/10.1016/S0191-8141(00)00053-5)  
805  
806 Bergantz, G. W., Schleicher, J. M. & Burgisser, A. (2015). Open system dynamics and mixing  
807 in magma mushes. *Nat Geosci.*, *8*, 793-797. <https://doi.org/10.1038/ngeo2534>  
808  
809 Bergantz, G.W., Schleicher, J.M. and Burgisser, A. (2017), On the kinematics and dynamics  
810 of crystal-rich systems, *Journal of Geophysical Research Solid Earth*, v. 122,  
811 [doi:10.1002/2017JB014218](https://doi.org/10.1002/2017JB014218)  
812  
813 Berlo, K., Blundy, J., Turner, S. & Hawkesworth, C. (2007). Textural and chemical variations  
814 in plagioclase phenocrysts from the 1980 eruptions of Mount St. Helens, USA. *Contrib. Mineral. Petrol.*, *154(3)*, 291-308. <https://doi.org/10.1007/s00410-007-0194-8>  
815  
816  
817 Bindeman I.N & Davis A.M (1999) Convection and redistribution of alkalis and trace elements during the mingling of basaltic and rhyolitic melts. *Petrol.*, *7(1)*, 91–101.  
818  
819  
820 Bindeman, I. N & Melnik, O. E. (2016). Zircon Survival, Rebirth and Recycling during Crustal Melting, Magma Crystallization, and Mixing Based on Numerical Modelling. *J. Petrol.*, *57(3)*, 437-460. <https://doi.org/10.1093/petrology/egw013>  
821  
822  
823  
824 Bindeman, I. N. & Simakin, A. G. (2014). Rhyolites – Hard to produce, but easy to recycle and sequester: Integrating microgeochemical observations and numerical models. *Geosphere*, *10(5)*, 930-957. <https://doi.org/10.1130/GES00969.1>  
825  
826  
827

828 Bishop, A. C. & French, W. J. (1982). Nature and origin of meladiorite layers in northern  
829 Guernsey, Channel Islands. *Mineral. Mag.*, 46(340), 301-321.  
830 <https://doi.org/10.1180/minmag.1982.046.340.03>  
831

832 Blake S. & Fink J. H. (1987) The dynamics of magma withdrawal from a density stratified  
833 dyke. *Earth. Planet. Sci. Lett.*, 85(4), 516–524. [https://doi.org/10.1016/0012-821X\(87\)90145-](https://doi.org/10.1016/0012-821X(87)90145-2)  
834 2  
835

836 Blundy, J. D. & Sparks, R. S. J. (1992). Petrogenesis of Mafic Inclusions in Granitoids of the  
837 Adamello Massif, Italy. *J. Petrol.*, 33(5), 1039-1104. [https://doi.org/10.1093/petrol-](https://doi.org/10.1093/petrology/33.5.1039)  
838 [ogy/33.5.1039](https://doi.org/10.1093/petrology/33.5.1039)  
839

840 Borisova, A. Y., Toutain, J., Dubessy, J., Pallister, J., Zwick, A. & Salvi, S. (2014). H<sub>2</sub>O-CO<sub>2</sub>-  
841 S fluid triggering the 1991 Mount Pinatubo climactic eruption (Philippines). *Bull. Volcanol.*,  
842 76, 800. <https://doi.org/10.1007/s00445-014-0800-3>  
843

844 Botcharnikov, R. E., Holtz, F., Almeev, R. R., Sato, H. & Behrens, H. (2008). Storage condi-  
845 tions and evolution of andesitic magma prior to the 1991-1995 eruption of Unzen volcano:  
846 Constraints from natural sample and phase equilibria experiments. *J. Volcanol. Geotherm.*  
847 *Res.*, 175(1-2), 168-180. <https://doi.org/10.1016/j.jvolgeores.2008.03.026>  
848

849 Bottinga, Y., Kudo, A. & Weill, D. (1966). Some observations on oscillatory zoning and  
850 crystallisation of magmatic plagioclase. *Am. Mineral.*, 51(5-6), 792-806.  
851

852 Browne, B. L., Eichelberger, J. C., Patino, L. C., Vogel, T. A., Dehn, J., Uto, K. & Hoshi-  
853 zumi, H. (2006a). Generation of Porphyritic and Equigranular Mafic Enclaves During  
854 Magma Recharge Events at Unzen Volcano, Japan. *J. Petrol.*, 47(2), 301-328.  
855 <https://doi.org/10.1093/petrology/egi076>  
856

857 Browne, B. L., Eichelberger, J. C., Patino, L. C., Vogel, T. A., Dehn, J., Uto, K. & Hoshi-  
858 zumi, H. (2006b). Magma mingling as indicated by texture and Sr/Ba ratios of plagioclase  
859 phenocrysts from Unzen volcano, SW Japan. *J. Volcanol. Geotherm. Res.*, 154(1-2), 103-116.  
860 <https://doi.org/10.1016/j.jvolgeores.2005.09.022>  
861

862 Bunsen, R. W. (1851). Über die Prozesse des vulkanischen Gesteinsbildungen Islands. *Ann.*  
863 *Phys. Chem. (Dritte Reihe)*, 83, 197-272.  
864

865 Campbell, I. H. & Turner, J. S. (1986). The Influence of Viscosity on Fountains in Magma  
866 Chambers. *J. Petrol.*, 27(1), 1-30. <https://doi.org/10.1093/petrology/27.1.1>  
867

868 Campbell, I. H. & Turner, J. S. (1989). Fountains in Magma Chambers. *J. Petrol.*, 30(4), 885-  
869 923. <https://doi.org/10.1093/petrology/30.4.885>  
870

871 Cantagrel, J., Didier, J. & Gourgaud, A. (1984). Magma mixing: origin of intermediate rocks  
872 and enclaves from volcanism to plutonism. *Phys. Earth Planet. Inter.*, 35(1-3), 63-76.  
873 [https://doi.org/10.1016/0031-9201\(84\)90034-7](https://doi.org/10.1016/0031-9201(84)90034-7)  
874

875 Cardoso, S. S. S. & Woods. A. W. (1996). Interfacial turbulent mixing in stratified magma  
876 reservoirs. *J. Volcanol. Geotherm. Res.*, 73(3-4), 157-175 [https://doi.org/10.1016/0377-](https://doi.org/10.1016/0377-0273(96)00028-5)  
877 [0273\(96\)00028-5](https://doi.org/10.1016/0377-0273(96)00028-5).

878

879 Caricchi, L., Burlini, L., Ulmer, P., Gerya, T., Vassalli, M. & Papale, P. (2007). Non-Newtonian rheology of crystal-bearing magmas and implications for magma ascent dynamics. *Earth Planet. Sci. Lett.*, 264(3-4), 402-419. <https://doi.org/10.1016/j.epsl.2007.09.032>

882

883 Caricchi, L., Annen, C., Rust, A. & Blundy, J. (2012). Insights into the mechanisms and time-scales of pluton assembly from deformation patterns of mafic enclaves, *J. Geophys. Res.*, 117, B11206. <https://doi.org/10.1029/2012JB009325>

886

887 Caroff, M., Coint, N., Hallot, E., Hamelin, C., Peucat, J. & Charreteur, G. (2011). The mafic-silicic layered intrusions of Saint-Jean du Doigt (France) and North Guernsey (Channel Islands), American Massif: Gabbro-diorite layering and mafic cumulate-pegmatoid association. *Lithos*, 125(1-2), 675-692. <https://doi.org/10.1016/j.lithos.2011.03.019>

891

892 Carrara, A., Burgisser, A. & Bergantz, G. W. (2019). Lubrication effects on magmatic mush dynamics. *J. Volcanol. Geotherm. Res.*, 380, 19-30. <https://doi.org/10.1016/j.jvolgeores.2019.05.008>

895

896 Carroll, M. R. & Wyllie, P. J. (1989). Granite melt convecting in an experimental micro-magma chamber at 1050 °C, 15 kbar. *Eur. J. Mineral.*, 1(2), 249-260.

898 DOI: [10.1127/ejm/1/2/0249](https://doi.org/10.1127/ejm/1/2/0249)

899

900 Carslaw, H. S. & Jaeger, J. C. (1959). *Conduction of Heat in Solids*. Oxford: Clarendon Press.

902

903 Cashman, K. & Blundy, J. (2000). Degassing and crystallization of ascending andesite and dacite. *Philos. Trans. Royal Soc. A*, 358(1770), 1487-1513. <https://doi.org/10.1098/rsta.2000.0600>

906

907 Cashman, K. & Blundy, J. (2013). Petrological cannibalism: The chemical and textural consequences of incremental magma body growth. *Contrib. Mineral. Petrol.*, 166(3), 703-729. <https://doi.org/10.1007/s00410-013-0895-0>

910

911 Cashman, K. V., Sparks, R. S. J. & Blundy, J. B., 2017. Vertically extensive and unstable magmatic systems: A unified view of igneous processes. *Science*, 355(6331), eaag3055. DOI: [10.1126/science.aag3055](https://doi.org/10.1126/science.aag3055)

914

915 Chamberlain, K. J., Morgan, D. J. & Wilson, C. J. N. (2014). Timescales of mixing and mobilisation in the Bishop Tuff magma body: perspectives from diffusion chronometry. *Contrib. Mineral. Petrol.*, 168, 1034. <https://doi.org/10.1007/s00410-014-1034-2>

918

919 Choe, W. & Jwa, Y. (2004). Petrological and geochemical evidences for magma mixing in the Palgongsan Pluton. *Geosci. J.*, 8, 343-354. <https://doi.org/10.1007/BF02910470>

921

922 Christopher, T. E., Humphreys, M. C. S., Barclay, J., Genereau, K., De Angelis, S. M. H., Plail, M. & Donovan, A. (2014). Petrological and geochemical variation during the Soufrière Hills eruption, 1995 to 2010. *Geol. Soc. Lond. Mem.*, 39, 317-342.

925 <https://doi.org/10.1144/M39.17>

926

927 Clynne, M A. (1990). Stratigraphic, lithogic and major element geochemical constrains on  
928 magmatic evolution at Lassen Volcanic Center, California. *J. Geophys. Res.*, 95(B12), 19651-  
929 19669. <https://doi.org/10.1029/JB095iB12p19651>  
930

931 Clynne, M. A. (1999). A Complex Magma Mixing Origin for Rocks Erupted in 1915, Lassen  
932 Peak, California. *J. Petrol.*, 40(1), 105-132. <https://doi.org/10.1093/ptroj/40.1.105>  
933

934 Coombs, M. L., Eichelberger, J. C. & Rutherford, M. J. (2000). Magma storage and mixing  
935 conditions for the 1953-1974 eruptions of Southwest Trident volcano, Katmai National Park,  
936 Alaska. *Contrib. Mineral. Petrol.*, 140(1), 99-118. <https://doi.org/10.1007/s004100000166>  
937

938 Coombs, M. L., Eichelberger, J. C. & Rutherford, M. J. (2002). Experimental and textural  
939 constraints on mafic enclave formation in volcanic rocks. *J. Volcanol. Geotherm. Res.*, 119(1-  
940 4), 125-144. [https://doi.org/10.1016/S0377-0273\(02\)00309-8](https://doi.org/10.1016/S0377-0273(02)00309-8)  
941

942 Cooper, K. M. (2017). What Does a Magma Reservoir Look Like? The “Crystal’s-Eye”  
943 View. *Elements*, 13(1), 23-29. <https://doi.org/10.2113/gselements.13.1.23>  
944

945 Cordonnier, B., K.-U. Hess, Y. Lavallée, and D. B. Dingwell (2009), Rheological properties  
946 of dome lavas: Case study of Unzen volcano, *Earth Planet. Sci. Lett.*, 279 (3–4), 263– 272,  
947 doi:10.1016/j.epsl.2009.01.014.  
948

949 d'Ars, J. B. & Davy, P. (1991). Gravity instabilities in magma chambers: rheological model-  
950 ling. *Earth Planet. Sci. Lett.*, 105(1-3), 319-329. [https://doi.org/10.1016/0012-](https://doi.org/10.1016/0012-821X(91)90140-D)  
951 [821X\(91\)90140-D](https://doi.org/10.1016/0012-821X(91)90140-D)  
952

953 Davidson, J. P., Morgan, D. J., Charlier, B. L. A., Harlou, R. & Hora, J. M. (2007). Mi-  
954 crosampling and Isotopic Analysis of Igneous Rocks: Implications for the Study of Magmatic  
955 Systems. *Annu. Rev. Earth Planet. Sci.*, 35, 273-311. [https://doi.org/10.1146/an-](https://doi.org/10.1146/annurev.earth.35.031306.140211)  
956 [nurev.earth.35.031306.140211](https://doi.org/10.1146/annurev.earth.35.031306.140211)  
957

958 De Campos, C. P., Dingwell, D. B. & Fehr, K. T. (2004). Decoupled convection cells from  
959 mixing experiments with alkaline melts from Phlegrean Fields. *Chem. Geol.*, 213, 227-251.  
960 <https://doi.org/10.1016/j.chemgeo.2004.08.045>  
961

962 De Campos, C. P., Dingwell, D. B., Perugini, D., Civetta, L., Fehr, T. K. (2008). Heterogene-  
963 ities in magma chambers : Insights from the behaviour of major and minor elements during  
964 mixing experiments with natural alkaline melts. *Chem. Geol.*, 256, 131-145.  
965 <https://doi.org/10.1016/j.chemgeo.2008.06.034>  
966

967 De Campos, C. P., Perugini, D., Ertel-Ingrisch, W., Dingwell, D. B., Poli, G. (2011). En-  
968 hancement of magma mixing efficiency by chaotic dynamics: an experimental study. *Con-*  
969 *trib. Mineral. Petrol.*, 161, 863-881. <https://doi.org/10.1007/s00410-010-0569-0>  
970

971 Diller, J. S. (1891). A late volcanic eruption in northern California and its peculiar lava. *Bul-*  
972 *letin of the U.S. Geological Survey*, 79.  
973

974 Dirksen, O., Humphreys, M. C. S., Pletchov, P., Melnik, O., Demyanchuk, Y. Sparks, R. S. J.  
975 & Mahony, S. (2006). The 2001-2004 dome-forming eruption of Shiveluch volcano, Kam-  
976 chatka: Observation, petrological investigation and numerical modelling. *J. Volcanol. Geo-*  
977 *therm. Res.*, 155(3-4), 201-226. <https://doi.org/10.1016/j.jvolgeores.2006.03.029>  
978  
979 D'Lemos, R. S. (1986). Interaction between co-existing magmas: field evidence from the  
980 Cobo Granite and the Bordeaux Diorite Complex, north-west Guernsey, Channel Islands.  
981 *Proc. Ussher*, 6, 323-329.  
982  
983 D'Lemos R. S. (1987) Relationships between the Cobo Granite and the Bordeaux Diorite  
984 Complex, Guernsey. (Doctoral dissertation). Retrieved from EThOS([https://ethos.bl.uk/Or-](https://ethos.bl.uk/OrderDetails.do?uin=uk.bl.ethos.304090)  
985 [derDetails.do?uin=uk.bl.ethos.304090](https://ethos.bl.uk/OrderDetails.do?uin=uk.bl.ethos.304090)) Oxford: Oxford Brookes University.  
986  
987 D'Lemos, R. S. (1996). Mixing between granitic and dioritic crystal mushes, Guernsey,  
988 Channel Islands, UK. *Lithos*, 38(3-4), 233-257. [https://doi.org/10.1016/0024-4937\(96\)00007-](https://doi.org/10.1016/0024-4937(96)00007-2)  
989 2  
990  
991 Druitt, T. H., Costa, F., Deloule, E., Dungan, M. & Scaillet, B. (2012). Decadal to monthly  
992 timescales of magma transfer and reservoir growth at a caldera volcano. *Nature*, 482, 77-80.  
993 <https://doi.org/10.1038/nature10706>  
994  
995 Edmonds, M., Kohn, S. C., Hauri, E. H., Humphreys, M. C. S. & Cassidy, M. (2016). Exten-  
996 sive, water-rich magma reservoir beneath southern Montserrat. *Lithos*, 252-253, 216-233.  
997 <https://doi.org/10.1016/j.lithos.2016.02.026>  
998  
999 Eichelberger, J. C. (1980). Vesiculation of mafic magma during the replenishment of silicic  
1000 magma reservoirs. *Nature*, 288, 446-450. <https://doi.org/10.1038/288446a0>  
1001  
1002 Einstein, A. (1906). Eine neue Bestimmung der Molekuldimensionen. *Ann. Phys.*, 324(2),  
1003 289-306. <https://doi.org/10.1002/andp.19063240204>  
1004  
1005 Elwell, R. W. D., Skelhorn, R. R. & Drysdall, A. R. (1960). Inclined Dioritic Pipes in the Di-  
1006 orites of Guernsey. *Geol. Mag.*, 97(2), 89-105. <https://doi.org/10.1017/S0016756800061215>  
1007  
1008 Elwell, R. W. D., Skelhorn, R. R. & Drysdall, A. R. (1962). Net-Veining in the Diorite of  
1009 Northeast Guernsey, Channel Islands. *J. Geol.*, 70(2), 215-226.  
1010 <https://doi.org/10.1086/626810>  
1011  
1012 Farrell, J., Smith, R. B., Husen, S. & Diehl, T. (2014). Tomography from 26 years of seismic-  
1013 ity revealing that the spatial extent of the Yellowstone crustal magma reservoir extends well  
1014 beyond the Yellowstone calder. *Geophys. Res. Lett.*, 41(9), 3068-3073.  
1015 <https://doi.org/10.1002/2014GL059588>  
1016  
1017 Fenner, C. N. (1926). The Katmai Magmatic Province. *J. Geol.*, 34(7 Part 2), 673-772.  
1018 <https://doi.org/10.1086/623350>  
1019  
1020 Folch, A. & Martí, J. (1998). The generation of overpressure in felsic magma chambers by  
1021 replenishment. *Earth Planet. Sci. Lett.*, 163, 301-314. [https://doi.org/10.1016/S0012-](https://doi.org/10.1016/S0012-821X(98)00196-4)  
1022 [821X\(98\)00196-4](https://doi.org/10.1016/S0012-821X(98)00196-4)  
1023

1024 Foley, F. V., Pearson, N. J., Rushmer, T., Turner, S. & Adam, J. (2012). Magmatic Evolution  
1025 and Magma Mixing of Quaternary Adakites at Solander and Little Solander Islands, New  
1026 Zealand. *J. Petrol.*, 54(4), 703-744. [https://doi.org/10.1093/](https://doi.org/10.1093/petrology/egs082)  
1027 petrology/egs082

1028 Fomin, S. & Plechov, P. Y. (2012). Exchange between Mafic Enclaves and Host Magma:  
1029 Case of 1991-1995 Mount Unzen Eruption. *J. Earth Sci. Engin.*, 2, 631-635.  
1030

1031 Francalanci, L., Avanzinelli, R., Nardini, I., Tiepolo, M., Davidson, J. P. & Vannucci, R.  
1032 (2011). Crystal recycling in the steady-state system of the active Stromboli volcano: a 2.5 ka  
1033 story inferred from in situ Sr-isotope and trace element data. *Contrib. Mineral. Petrol.*, 163,  
1034 109-131. <https://doi.org/10.1007/s00410-011-0661-0>  
1035

1036 Frost, T. P. & Mahood, G. A. (1987). Field. Chemical and physical constraints on mafic-fel-  
1037 sic interaction in the Lamarck Granodiorite, Sierra Nevada, California. *Geol. Soc. Am. Bull.*,  
1038 99(2), 272-291. [https://doi.org/10.1130/0016-7606\(1987\)99%3C272:FCAPCO%3E2.0.CO;2](https://doi.org/10.1130/0016-7606(1987)99%3C272:FCAPCO%3E2.0.CO;2)  
1039

1040 Giordano, D., Russel, J. K. & Dingwell, D. B. (2008). Viscosity of magmatic liquids: A  
1041 model. *Earth Planet. Sci. Lett.*, 271, 123-134. <https://doi.org/10.1016/j.epsl.2008.03.038>  
1042

1043 Gourgaud, A. & Maury, R. C. (1984). Magma mixing in Alkaline Series: an Example from  
1044 Sancy Volcano (More-Dore, Massif Central, France). *Bull. Volcanol.*, 47(4), 827-848.  
1045 <https://doi.org/10.1007/BF01952346>  
1046

1047 Grasset O. & Albarède F. (1994). Hybridization of mingling magmas with different densities.  
1048 *Earth Planet. Sci. Lett.*, 121(3-4), 327-332. [https://doi.org/10.1016/0012-821X\(94\)90075-2](https://doi.org/10.1016/0012-821X(94)90075-2)  
1049

1050 Grove, T. L., Baker, M. B. & Kinzler, R. J. (1984). Coupled CaAl-NaSi diffusion in plagi-  
1051 clase feldspar: Experiments and applications to cooling rate speedometry. *Geochem. Cosmo-*  
1052 *chem. Acta*, 48(10), 3785-3793. [https://doi.org/10.1016/0016-7037\(84\)90391-0](https://doi.org/10.1016/0016-7037(84)90391-0)  
1053

1054 Harker, A. (1909). *The Natural History of Igneous Rocks*. Cambridge: Cambridge University  
1055 Press.  
1056

1057 Heiken, G. & Eichelberger, J. C. (1980). Eruptions at Chaos Crags, Lassen Volcanic National  
1058 Park, California. *J. Volcanol. Geotherm. Res.*, 7(3-4), 443-481. [https://doi.org/10.1016/0377-](https://doi.org/10.1016/0377-0273(80)90042-6)  
1059 [0273\(80\)90042-6](https://doi.org/10.1016/0377-0273(80)90042-6)  
1060

1061 Hibbard, M. J. (1981). The Magma Mixing Origin of Mantled Feldspars. *Contrib. Mineral.*  
1062 *Petrol.*, 76(2), 158-170. <https://doi.org/10.1007/BF00371956>  
1063

1064 Hiess, J., Cole, J. W., & Spinks, K. D. (2007). Influence of the crust and crustal structure on  
1065 the location and composition of high-alumina basalts of the Taupo Volcanic Zone, New Zea-  
1066 land. *New Zeal. J. Geol. Geop.*, 50(4), 327-342. <https://doi.org/10.1080/00288300709509840>  
1067

1068 Hildreth, W. (1981). Gradients in silicic magma chambers: implications for lithospheric mag-  
1069 matism. *J. Geophys. Res.*, 86, 10153-10192. <https://doi.org/10.1029/JB086iB11p10153>  
1070

1071 Hildreth, W. (2004). Volcanological perspectives on Long Valley, Monmouth Mountain, and  
1072 Mono Craters: several contiguous but discrete systems. *J. Volcanol. Geotherm. Res.*, 136(3-  
1073 4), 169-198. <https://doi.org/10.1016/j.jvolgeores.2004.05.019>

1074  
1075 Hodge, K. F., Carazzo, G. & Jellinek, A. M. (2012). Experimental constraints on the defor-  
1076 mation and breakup of injected magma. *Earth Planet. Sci. Lett.*, 325-326, 52-62.  
1077 <https://doi.org/10.1016/j.epsl.2012.01.031>  
1078  
1079 Hodge, K. F. & Jellinek, A. M. (2012). Linking enclave formation to magma rheology. *J. Ge-*  
1080 *ophys. Res.*, 117(B10), 208. <https://doi.org/10.1029/2012JB009393>  
1081  
1082 Holtz, F., Sato, H., Lewis, J., Behrens, H. & Nakada, S. (2005). Experimental Petrology of  
1083 the 1991-1995 Unzen Dacite, Japan. Part I: Phase relations, Phase Composition and Pre-erup-  
1084 tive Conditions. *J. Petrol.*, 46(2), 319-337. [https://doi.org/10.1093/](https://doi.org/10.1093/petrology/egh077)  
1085 [petrology/egh077](https://doi.org/10.1093/petrology/egh077)  
1086 Hornby, A. J., Kendrick, J. E., Lamb, O. D., Hirose, T., De Angelis, S., von Aulock, F. W.,  
1087 Umakoshi, K., Miwa, T., Henton De Angelis, S., Wadsworth, F. B., Hess, K.-U., Dingwell,  
1088 D. B., and Lavallée, Y. (2015), Spine growth and seismogenic faulting at Mt. Unzen, Japan.  
1089 *J. Geophys. Res. Solid Earth*, 120, 4034–4054. doi: 10.1002/2014JB011660.  
1090  
1091 Hoshzumi, H., Uto, K. & Watanabe, K., 1999. Geology and eruptive history of Unzen vol-  
1092 cano, Shimbara Peninsula, Kyushu, SW Japan. *J. Volcanol. Geotherm. Res.*, 89(1-4), 81-94.  
1093 [https://doi.org/10.1016/S0377-0273\(98\)00125-5](https://doi.org/10.1016/S0377-0273(98)00125-5)  
1094  
1095 Humphreys, M. C. S., Blundy, J. D. & Sparks, R. S. J. (2006). Magma Evolution and Open-  
1096 System Processes at Shiveluch Volcano: Insights from Phenocryst Zoning. *J. Petrol.*, 47(12),  
1097 2303-2334. [https://doi.org/10.1093/](https://doi.org/10.1093/petrology/egl045)  
1098 [petrology/egl045](https://doi.org/10.1093/petrology/egl045)  
1099 Humphreys, M. C. S., Christopher, T. & Hards, V. (2009). Microlite transfer by disaggrega-  
1100 tion of mafic inclusions following magma mixing at Soufrière Hills volcano, Montserrat.  
1101 *Contrib. Mineral. Petrol.*, 157(5), 609-624. <https://doi.org/10.1007/s00410-008-0356-3>  
1102  
1103 Humphreys M. C. S., Edmonds M., Christopher T. & Hards, V. (2010). Magma hybridisation  
1104 and diffusive exchange recorded in heterogeneous glasses from Soufrière Hills Volcano,  
1105 Montserrat. *Geophys. Res. Lett.*, 37(19). <https://doi.org/10.1029/2009GL041926>  
1106  
1107 Huppert, H. E., Sparks, R. S. J. S. & Turner, J. S. (1984). Some effects of viscosity on the dy-  
1108 namics of replenished magma chambers. *J. Geophys. Res.*, 89(B8), 6857-6877.  
1109 <https://doi.org/10.1029/JB089iB08p06857>  
1110  
1111 Huppert, H. E., Sparks, R. S. J., Whitehead, J. A. & Hallworth, M. A. (1986). Replenishment  
1112 of Magma Chambers by Light Inputs. *J. Geophys. Res.*, 91(B6), 6113-6122.  
1113 <https://doi.org/10.1029/JB091iB06p06113>  
1114  
1115 Iddings, J. P. (1890). A group of volcanic rocks from the Tewan Mountains, New Mexico,  
1116 and on the occurrence of primary quartz in certain basalts. *Bulletin of the U.S. Geological*  
1117 *Survey*, 66.  
1118  
1119 Ishii, M. & Zuber, N. (1979). Drag coefficient and relative velocity in bubbly, droplet or par-  
1120 ticulate flows. *AiChE Journal*, 25(5), 843-855. <https://doi.org/10.1002/aic.690250513>  
1121  
1122 Jackson, M. D. & Cheadle, M. J. (1998). A continuum model for the transport of heat, mass  
1123 and momentum in a deformable, multicomponent mush, undergoing solid-liquid phase

1124 change. *Int. J. Heat Mass Transf.*, 41(8-9), 1035-1048. <https://doi.org/10.1016/S0017->  
1125 9310(97)00197-X  
1126  
1127 Janoušek, C., Braithwaite, C. J. R., Bowes, D. R. & Gerdes, A. (2004). Magma-mixing in the  
1128 genesis of Hercynian calc-alkaline granitoids: an integrated petrographic and geochemical  
1129 study of the sázava intrusion, Central Bohemian Pluton, Czech Republic. *Lithos*, 78(1-2), 67-  
1130 99. <https://doi.org/10.1016/j.lithos.2004.04.046>  
1131  
1132 Jarvis, P. A., Mader, H. M., Huppert, H. E., Cashman, K. V. & Blundy, J. D. (2019). Experi-  
1133 ments on the low-Reynolds number settling of a sphere through a fluid interface. *Phys. Rev.*  
1134 *Fluids*, 4, 024003. <https://doi.org/10.1103/PhysRevFluids.4.024003>  
1135  
1136 Judd, J. W. (1893). On composite dykes in Arran. *Q. J. Geol. Soc. Lond.*, 49, 536-565.  
1137 <https://doi.org/10.1144/GSL.JGS.1893.049.01-04.63>  
1138  
1139 Kerr, R. C. (1994). Melting driven by vigorous compositional convection. *J. Fluid Mech.*,  
1140 280, 255-285. <https://doi.org/10.1017/S0022112094002922>  
1141  
1142 Kim, J., Shin, K. & Lee, J. D. (2002). Petrographical study on the Yucheon granite and its en-  
1143 claves. *Geosci. J.*, 6, 289-302. <https://doi.org/10.1007/BF03020614>  
1144  
1145 Kim, J., Son, M., Hwang, B., Shin, K., Cho, H. & Sohn, Y. K. (2014). Double injection  
1146 events of mafic magmas into supersolidus Yucheon granites to produce two types of mafic  
1147 enclaves in the Cretaceous Gyeongsang Basin, SE Korea. *Mineral. Petrol.*, 108(2), 207-229.  
1148 <https://doi.org/10.1007/s00710-013-0296-0>  
1149  
1150 King, B. C. (1964). The nature of basic igneous rocks and their relations with associated acid  
1151 rocks. Part IV. *Sci. Prog.*, 52(206), 282-292.  
1152  
1153 Koyaguchi, T. & Blake, S. (1989) The dynamics of magma mixing in a rising magma batch.  
1154 *Bull. Volcanol.* 52(2), 127–137. <https://doi.org/10.1007/BF00301552>  
1155  
1156 Kouchi, A. & Sunagawa, I. (1983). Mixing basaltic and dacitic magmas by forced convec-  
1157 tion. *Nature*, 304, 527-528. <https://doi.org/10.1038/304527a0>  
1158  
1159 Kouchi, A. & Sunagawa, I. (1985). A model for mixing basaltic and dacitic magmas as de-  
1160 duced from experimental data. *Contrib. Mineral. Petrol.*, 89(1), 17-23.  
1161 <https://doi.org/10.1007/BF01177586>  
1162  
1163 Kumar, S. & Rino, V. (2006). Mineralogy and geochemistry of microgranular enclaves in  
1164 Paleoproterozoic Malanjkhand granitoids, central India: evidences of magma mixing, min-  
1165 gling and chemical equilibration. *Contrib. Mineral. Petrol.*, 152, 591-609.  
1166 <https://doi.org/10.1007/s00410-006-0122-3>  
1167  
1168 Larsen, L. L. & Smith, E. I. (1990). Mafic Enclaves in the Wilson Ridge Pluton, Northwest-  
1169 ern Arizona: Implications for the Generation of a Calc-Alkaline Intermediate Pluton in an Ex-  
1170 tension Environment. *J. Geophys. Res.*, 95(B11), 17693-17716.  
1171 <https://doi.org/10.1029/JB095iB11p17693>  
1172

1173 Laumonier, M., Scaillet, B., Arbaret, L. & Champallier, R. (2014). Experimental simulation  
1174 of magma mixing at high pressure. *Lithos*, 196-197, 281–300. <https://doi.org/10.1016/j.lithos.2014.02.016>  
1175  
1176

1177 Laumonier, M., Scaillet, B., Arbaret, L., Andújar, J. & Champallier, R. (2015). Experimental  
1178 mixing of hydrous magmas. *Chem. Geol.*, 418, 158-170.  
1179 <https://doi.org/10.1016/j.chemgeo.2015.10.031>  
1180

1181 Leonard, G. S., Cole, J. W., Nairn, I. A. & Self, S. (2002). Basalt triggering of the c. AD  
1182 1305 Kaharoa rhyolite eruption, Tarawere Volcanic Complex, New Zealand. *J. Volcanol. Ge-*  
1183 *otherm. Res.*, 115(3-4), 461-486. [https://doi.org/10.1016/S0377-0273\(01\)00326-2](https://doi.org/10.1016/S0377-0273(01)00326-2)  
1184

1185 Leshner C. E. (1994) Kinetics of Sr and Nd exchange in silicate liquids: theory, experiments,  
1186 and applications to uphill diffusion, isotopic equilibration, and irreversible mixing of mag-  
1187 mas. *J. Geophys. Res.*, 99(B5), 9585–9604. <https://doi.org/10.1029/94JB00469>  
1188

1189 Lipman, P., Dungan, M. & Bachmann, O. (1997). Comagmatic granophyre granite in the Fish  
1190 Canyon Tuff, Colorado: Implications for magma-chamber processes during a large ash-flow  
1191 eruption. *Geology*, 25(10), 915-918. [https://doi.org/10.1130/0091-](https://doi.org/10.1130/0091-7613(1997)025%3C0915:CGGITF%3E2.3.CO;2)  
1192 [7613\(1997\)025%3C0915:CGGITF%3E2.3.CO;2](https://doi.org/10.1130/0091-7613(1997)025%3C0915:CGGITF%3E2.3.CO;2)  
1193

1194 Litvinovsky, B. A., Zanzivilevich, A. N. & Katzir, Y. (2012). Formation of composite dykes by  
1195 contact remelting and magma mingling: The Shaluta pluton, Transbaikalia (Russia). *J. Asian*  
1196 *Eart Sci.*, 60, 18-30. <https://doi.org/10.1016/j.jseaes.2012.07.018>  
1197

1198 Mader, H. M., Llewellyn, E. W. & Mueller, S. P. (2013). The rheology of two phase magmas:  
1199 A review and analysis. *J. Volcanol. Geotherm. Res.*, 257, 135-158.  
1200 <https://doi.org/10.1016/j.jvolgeores.2013.02.014>  
1201

1202 Martel C., Ali R.A., Poussineau S., Gourgaud A. & Pichavant M. (2006) Basalt-inherited mi-  
1203 crolites in silicic magmas: Evidence for Mount Pelée (Martinique, French West Indies), *Geol-*  
1204 *ogy*, 34, 905-908. <https://doi.org/10.1130/G22672A.1>  
1205

1206 Martin, V. M, Pyle, D. M. & Holness, M. B. (2006). The role of crystal frameworks in the  
1207 preservation of enclaves during magma mixing. *Earth Planet. Sci. Lett.*, 248(3-4), 787-799.  
1208 <https://doi.org/10.1016/j.epsl.2006.06.030>  
1209

1210 Matthews, S. J., Jones, A. P. & Bristow, C. S. (1992). A simple magma-mixing model for  
1211 sulphur behaviour in calc-alkaline volcanic rocks: mineralogical evidence from Mount  
1212 Pinatubo 1991 eruption. *J. Geol. Soc.*, 149, 863-866. <https://doi.org/10.1144/gsjgs.149.6.0863>  
1213

1214 Matthews, S. J., Jones, A. P. & Gardeweg, M. C. (1994). Lascar Volcano, Northern Chile;  
1215 Evidence for Steady-State Disequilibrium. *J. Petrol.*, 35(2), 401-432.  
1216 <https://doi.org/10.1093/petrology/35.2.401>  
1217

1218 McCormick Kilbride, B., Biggs, J., Edmonds, M., (2016). Observing eruptions of gas-rich  
1219 compressible magmas from space. *Nat. Commun.*, 7, 13744.  
1220 <https://doi.org/10.1038/ncomms13744>  
1221

1222 McIntire, M.Z., Bergantz, G.W. & Schleicher, J.M. (2019), On the hydrodynamics of crystal  
1223 clustering, *Philos. Trans. Royal Soc. A*, 377(2139), 20180015.  
1224 <https://doi.org/10.1098/rsta.2018.0015>  
1225

1226 Miller, D.S., & Smith, R.B. (1999), P and S velocity structure of the Yellowstone volcanic  
1227 field from local earthquake and controlled source tomography, *J. Geophys. Res.*, 104(B7),  
1228 15105–15121. <https://doi.org/10.1029/1998JB900095>  
1229

1230 Mollo, S., Putirka, K., Iezzi, G., Del Gaudio, P. & Scarlato, P. (2011) Plagioclase-melt  
1231 (dis)equilibrium due to cooling dynamics: Implications for thermometry, barometry and hy-  
1232 grometry, *Lithos*, 125, 221-235. <https://doi.org/10.1016/j.lithos.2011.02.008>  
1233

1234 Montagna, C. P., Papale, P. & Longo, A. (2015). Timescales of mingling in shallow mag-  
1235 matic reservoirs. *Geol. Soc. Spec. Pub.*, 422, 131-140. <https://doi.org/10.1144/SP422.6>  
1236

1237 Morgan, G. B., Acosta-Vigil, A. & London, D. (2008) Diffusive equilibration between hy-  
1238 drous metaluminous-peraluminous haplogranite liquid couples at 200 MPa (H<sub>2</sub>O) and alkali  
1239 transport in granitic liquids. *Contrib. Mineral. Petrol.*, 155(2), 257–269.  
1240 <https://doi.org/10.1007/s00410-007-0242-4>  
1241

1242 Morgavi, D., Arienzo, I., Montagna, C., Perugini, D. & Dingwell, D. B. (2019). Magma mix-  
1243 ing: History and dynamics of an eruption trigger. In *Volcanic Unrest* (123-137). Springer,  
1244 Cham.  
1245

1246 Morgavi, D., Arzilli, F., Pritchard, C., Perugini, D., Mancini, L., Larson, P. & Dingwell, D.  
1247 B. (2016). The Grizzly Lake complex (Yellowstone Volcano, USA): Mixing between basalt  
1248 and rhyolite unravelled by microanalysis and X-ray microtomography. *Lithos*, 260, 457-474.  
1249 <https://doi.org/10.1016/j.lithos.2016.03.026>  
1250

1251 Morgavi, D., Perugini, D., De Campos, C. P., Ertl-Ingrisch, W., Lavalée, Y., Morgan, L. &  
1252 Dingwell, D. B. (2013). Interactions between rhyolitic and basaltic melts unraveled by cha-  
1253 otic mixing experiments. *Chem Geol.*, (346), 199-212.  
1254 <https://doi.org/10.1016/j.chemgeo.2012.10.003>  
1255

1256 Morse, S. A. (1984). Cation Diffusion in Plagioclase Feldspar. *Science*, 225(4661), 504-505.  
1257 DOI: 10.1126/science.225.4661.504  
1258

1259 Mueller, S., Llewellyn, E. W. & Mader, H. M. (2009). The rheology of suspensions of solid  
1260 particles. *Proc. Royal Soc. Lond.*, 466(2116), 1201-1228.  
1261 <https://doi.org/10.1098/rspa.2009.0445>  
1262

1263 Murphy, M. D., Sparks, R. S. J., Barclay, J., Carroll, M. R. & Brewer, T. S. (2000). Remobi-  
1264 lisation of Andesite Magma by Intrusion of Mafic Magma at the Soufriere Hills Volcano,  
1265 Montserrat, West Indies. *J. Petrol.*, 41(1), 21-42. <https://doi.org/10.1093/petrology/41.1.21>  
1266

1267 Nakada, S. & Fujii, T. (1993). Preliminary report on the activity at Unzen Volcano (Japan),  
1268 November 1990 – November 1991: Dacite lava domes and pyroclastic flows. *J. Volcanol.*  
1269 *Geotherm. Res.*, 54(3-4), 319 – 333. [https://doi.org/10.1016/0377-0273\(93\)90070-8](https://doi.org/10.1016/0377-0273(93)90070-8)  
1270

1271 Nakada, S. & Motomura, Y. (1999). Petrology of the 1991-1995 eruption at Unzen: effusion  
1272 pulsation and groundmass crystallization. *J. Volcanol. Geotherm. Res.*, 89(1-4), 173-196.  
1273 [https://doi.org/10.1016/S0377-0273\(98\)00131-0](https://doi.org/10.1016/S0377-0273(98)00131-0)  
1274

1275 Nakada, S., Shimizu, H. & Ohta, K., 1999. Overview of the 1991-1995 eruption at Unzen  
1276 Volcano. *J. Volcanol. Geotherm. Res.*, 89(1-4), 1-22. [https://doi.org/10.1016/S0377-](https://doi.org/10.1016/S0377-0273(98)00118-8)  
1277 0273(98)00118-8  
1278

1279 Nakamura, E. & Kushiro I. (1998). Trace element diffusion in jadeite and diopside melts at  
1280 high pressures and its geological implication. *Geochim. Cosmochim. Acta*, 62(18), 3151-  
1281 3160. [https://doi.org/10.1016/S0016-7037\(98\)00223-3](https://doi.org/10.1016/S0016-7037(98)00223-3)  
1282

1283 Nakamura, M. & Shimakita, S. (1998). Dissolution origin and syn-entrapment compositional  
1284 change of melt inclusions in plagioclase. *Earth Planet. Sci. Lett.*, 161(1-4), 119-133.  
1285 [https://doi.org/10.1016/S0012-821X\(98\)00144-7](https://doi.org/10.1016/S0012-821X(98)00144-7)  
1286

1287 Nandedekar, R. H., Ulmer, P. & Müntener, O. (2014). Fractional crystallisation of primitive,  
1288 hydrous arc magmas: an experimental study at 0.7 GPa. *Contrib. Mineral. Petrol.*, 167, 1015.  
1289 <https://doi.org/10.1007/s00410-014-1015-5>  
1290

1291 Neill, O. K., Larsen, J. F., Izbekov, P. E. & Nye, C. J. (2015). Pre-eruptive magma mixing  
1292 and crystal transfer revealed by phenocryst and microlite compositions in basaltic andesite  
1293 from the 2008 eruption of Kasatochi Island volcano. *Am. Mineral.*, 100(4), 722-737.  
1294 <https://doi.org/10.2138/am-2015-4967>  
1295

1296 Nockolds, S. R. (1933). Some Theoretical Apects of Contamination in Acid Magmas. *J.*  
1297 *Geol*, 41(6), 561-589. <https://doi.org/10.1086/624072>  
1298

1299 Oldenburg, C. M., Spera, F. J., Yuen, D. A. & Sewell, G. (1989) Dynamic mixing in magma  
1300 bodies: theory, simulations and implications. *J. Geophys. Res.*, 94(B7), 9215–9236.  
1301 <https://doi.org/10.1029/JB094iB07p09215>  
1302

1303 Oppenheimer, J., Rust, A. C., Cashman, K. V. & Sandnes, B. (2015). Gas migration regimes  
1304 and outgassing in particle-rich suspensions. *Front. Phys.*, 3, 60.  
1305 <https://doi.org/10.3389/fphy.2015.00060>  
1306

1307 Papale, P., Montagna, C. P. & Longo, A. (2017). Pressure evolution in shallow magma cham-  
1308 bers upon buoyancy driven replenishment. *Geochem. Geophys. Geosyst.*, 18, 1214-1224.  
1309 <https://doi.org/10.1002/2016GC006731>  
1310

1311 Papale, P., Moretti, R. & Barbato, D. (2006). The compositional dependence of the saturation  
1312 surface of H<sub>2</sub>O + CO<sub>2</sub> fluids in a silicate melt. *Chem. Geol.*, 229(1-3), 78-95.  
1313 <https://doi.org/10.1016/j.chemgeo.2006.01.013>  
1314

1315 Perugini, D., De Campos, C. P., Dingwell, D. P. & Dorfman, A. (2013). Relaxation of con-  
1316 centration variance: A new tool to measure chemical element variability during mixing of  
1317 magmas. *Chem. Geol.*, 335, 8-23. <https://doi.org/10.1016/j.chemgeo.2012.10.050>  
1318

1319 Perugini, D., De Campos, C. P., Dingwell, D. B., Petrelli, M. & Poli, G. (2008). Trace ele-  
1320 ment mobility during magma mixing: Preliminary experimental results. *Chem. Geol.*, 256(3-  
1321 4), 146-157. <https://doi.org/10.1016/j.chemgeo.2008.06.032>  
1322

1323 Perugini, D., De Campos, C. P., Ertel-Ingrisch, W. & Dingwell, D. B. (2012). The space and  
1324 time complexity of mixing silicate melts: Implications for igneous petrology. *Lithos*, 155,  
1325 326-340. <https://doi.org/10.1016/j.lithos.2012.09.010>  
1326

1327 Perugini, D., De Campos, C. P., Petrelli, M., Morgavi, D., Vetere, F. P. & Dingwell, D. B.  
1328 (2015). Quantifying magma mixing with the Shannon entropy: Application to simulations  
1329 and experiments. *Lithos*, 236-237, 299-310. <https://doi.org/10.1016/j.lithos.2015.09.008>  
1330

1331 Perugini, D. & Poli, G. (2004). Analysis and numerical simulation of chaotic advection and  
1332 chemical diffusion during magma mixing: petrological implications. *Lithos* 78(1-2), 43–66.  
1333 <https://doi.org/10.1016/j.lithos.2004.04.039>  
1334

1335 Perugini, D. & Poli, G. (2005). Viscous fingering during replenishment of felsic magma  
1336 chambers by continuous inputs of mafic magmas: Field evidence and fluid mechanics experi-  
1337 ments. *Geology*, 33(1), 5-8. <https://doi.org/10.1130/G21075.1>  
1338

1339 Perugini, D. & Poli, G. (2012). The mixing of magmas in plutonic and volcanic environ-  
1340 ments: Analogies and differences. *Lithos*, 153, 261-277. [https://doi.org/10.1016/j.li-](https://doi.org/10.1016/j.lithos.2012.02.002)  
1341 [thos.2012.02.002](https://doi.org/10.1016/j.lithos.2012.02.002)  
1342

1343 Perugini, D., Poli, G., Christofides, G. & Eleftheriadis, G. (2003). Magma mixing in the  
1344 Sithonia Plutonic Complex, Greece: evidence from mafic microgranular enclaves. *Mineral.*  
1345 *Petrol.*, 78(3-4), 173-200. <https://doi.org/10.1007/s00710-002-0225-0>  
1346

1347 Perugini, D., Valentini, L. & Poli, G. (2007). Insights into magma chamber processes from  
1348 the analysis of size distributions of enclaves in lava flows: A case study from Vulcano Island  
1349 (Southern Italy). *J. Volcanol. Geotherm. Res.*, 166(3-4), 193-203.  
1350 <https://doi.org/10.1016/j.jvolgeores.2007.07.017>  
1351

1352 Petrelli, M., El Omari, K., Spina, L., Le Guer, Y., La Spina, G. & Perugini, D. (2018). Time-  
1353 scales of water accumulation in magmas and implications for short warning times of explo-  
1354 sive eruptions. *Nat. Commun.*, 9(1), 1-14. <https://doi.org/10.1038/s41467-018-02987-6>  
1355

1356 Petrelli, M., Perugini, D. & Poli, G. (2006). Timescales of hybridisation of magmatic en-  
1357 claves in regular and chaotic flow fields: petrologic and volcanologic implications. *Bull.*  
1358 *Volc.*, 68, 285-293. <https://doi.org/10.1007/s00445-005-0007-8>  
1359

1360 Phillips, J. A. (1880). On concretionary patches and fragments of other rocks contained in  
1361 granite. *Q. J. Geol. Soc. Lond.*, 36, 1-22. <https://doi.org/10.1144/GSL.JGS.1880.036.01-04.03>  
1362

1363 Phillips, J. C. & Woods A. W. (2001). Bubble plumes generated during recharge of basaltic  
1364 magma reservoirs. *Earth Planet. Sci. Lett.*, 186(2), 297-309. [https://doi.org/10.1016/S0012-](https://doi.org/10.1016/S0012-821X(01)00221-7)  
1365 [821X\(01\)00221-7](https://doi.org/10.1016/S0012-821X(01)00221-7)  
1366

1367 Pin, C., Binon, M., Belin, J. M., Barbarin, B. & Clemens, J. D. (1990). Origin of Microgranu-  
1368 lar Enclaves in Granitoids: Equivocal Sr-Nd Evidence from Hercynian Rocks in the Massif

1369 Central (France). *J. Geophys. Res.*, 95(B11), 17821-17828.  
1370 <https://doi.org/10.1029/JB095iB11p17821>  
1371  
1372 Pistone, M., Caricchi, L., Ulmer, P., Burlini, L., Ardia, P., Reusser, E., Marone, F. & Arbaret,  
1373 L., 2012. Deformation experiments of bubble and crystal-bearing magmas: rheological and  
1374 microstructural analysis. *J. Geophys. Res.*, 117(B5). <https://doi.org/10.1029/2011JB008986>  
1375  
1376 Pistone, M., Blundy, J. D., Brooker, R. A. & EIMF (2016a). Textural and chemical conse-  
1377 quences of interaction between hydrous and felsic magmas: an experimental study. *Contrib.*  
1378 *Mineral. Petrol.*, 171(1), 8. <https://doi.org/10.1007/s00410-015-1218-4>  
1379  
1380 Pistone M, Cordonnier B, Ulmer P, Caricchi L (2016b). Rheological flow laws for multi-  
1381 phase magmas: an empirical approach. *Journal of Volcanology and Geothermal Research*,  
1382 321, 158-170, <https://doi.org/10.1016/j.jvolgeores.2016.04.029>  
1383  
1384 Pistone, M., Blundy, J. & Brooker, R. A. (2017). Water transfer during magma mixing  
1385 events: Insights into crystal mush rejuvenation and melt extraction processes. *Am. Mineral.*,  
1386 102(4), 766-776. <https://doi.org/10.2138/am-2017-5793>  
1387  
1388 Plail, M., Barclay, J., Humphreys, M. C. S., Edmonds, M., Herd, R. A. & Christopher, T. E.  
1389 (2014). Characterization of mafic enclaves in the erupted products of Soufrière Hills Vol-  
1390 cano, Montserrat, 2009 to 2010. *Geol. Soc. Lond. Mem.*, 39, 343-360.  
1391 <https://doi.org/10.1144/M39.18>  
1392  
1393 Plail, M., Edmonds, E., Woods, A. W., Barclay, J., Humphreys, M. C. S., Herd, R. A. &  
1394 Christopher, T. (2018). Mafic enclaves record syn-eruptive basalt intrusion and mixing. *Earth*  
1395 *Planet. Sci. Lett.*, 484, 30-40. <https://doi.org/10.1016/j.epsl.2017.11.033>  
1396  
1397 Prelević, D., Foley, S. F., Cvetković, V. & Romer, R. L. (2004). Origin of Minette by Mixing  
1398 of Lamproite and Dacite Magmas in Veliki Majdan, Serbia. *J. Petrol.*, 45(4), 759-792.  
1399 <https://doi.org/10.1093/petrology/egg109>  
1400  
1401 Pritchard, M. E., de Silva, S. L., Michelfelder, G., Zandt, G., McNutt, S. R., Gottsmann, J., et  
1402 al. (2018). Synthesis: PLUTONS: Investigating the relationship between pluton growth and  
1403 volcanism in the Central Andes. *Geosphere*, 14(3), 954-982.  
1404 <https://doi.org/10.1130/GES01578.1>  
1405  
1406 Reagan, M. K., Gill, J. B., Malavassi, E. & Garcia, M. O. (1987). Changes in magma compo-  
1407 sition at Arenal volcano, Costa Rica, 1968-1985: Real-time monitoring of open-system dif-  
1408 ferentiation. *Bull. Volcanol.*, 49, 415-434. <https://doi.org/10.1007/BF01046634>  
1409 Reid, J. B., Evans, O. & Fates, D. G. (1983). Magma mixing in granitic rocks of the central  
1410 Sierra Nevada, California. *Earth Planet. Sci. Lett.*, 66, 243-261. [https://doi.org/10.1016/0012-](https://doi.org/10.1016/0012-821X(83)90139-5)  
1411 [821X\(83\)90139-5](https://doi.org/10.1016/0012-821X(83)90139-5)  
1412  
1413 Renggli, C. J., Wiesmaier, S., De Campos, C. P., Hess, K. & Dingwell, D. B. (2016). Magma  
1414 mixing induced by particle settling. *Contrib. Mineral. Petrol.*, 171, 96.  
1415 <https://doi.org/10.1007/s00410-016-1305-1>  
1416  
1417 Roscoe, R. (1952). The viscosity of suspensions of rigid spheres. *Br. J. Appl. Phys.*, 3(8),  
1418 267–269. <https://doi.org/10.1088/0508-3443/3/8/306>

1419  
1420 Rossi, S., Petrelli, M., Morgavi, D., Vetere, F. P., Almeev, R. R., Astbury, R. L. & Perugini,  
1421 D. (2019). Role of magma mixing in the pre-eruptive dynamics of the Aeolian Islands volca-  
1422 noes (Southern Tyrrhenian Sea, Italy). *Lithos*, 324-325, 165-179. <https://doi.org/10.1016/j.lithos.2018.11.004>  
1423  
1424  
1425 Ruprecht, P. & Wörner, G. (2007). Variable regimes in magma systems documented in plagi-  
1426 oclase zoning patterns: El Misti stratovolcano and Andahua monogenetic cones. *J. Volcanol.*  
1427 *Geotherm. Res.*, 165(3-4), 142-162. <https://doi.org/10.1016/j.jvolgeores.2007.06.002>  
1428  
1429 Ruprecht, P., Bergantz, G. W., Cooper, K. M. & Hildreth, W. (2012). The Crustal Magma  
1430 Storage System of Volcán Quizapu, Chile, and the Effects of Magma Mixing on Magma Di-  
1431 versity. *J. Petrol.*, 53(4), 801-840. <https://doi.org/10.1093/petrology/egs002>  
1432  
1433 Şahin, S. Y. (2008). Geochemistry of mafic microgranular enclaves in the Tamdere Quartz  
1434 Monzonite, south of Dereli/Giresum, Eastern Pontides, Turkey. *Chem. Erde-Geochem.*,  
1435 68(1), 81-92. <https://doi.org/10.1016/j.chemer.2005.05.002>  
1436  
1437 Samaniego, P., Le Pennec, J., Robin, C. & Hidalgo, S. (2011). Petrological analysis of the  
1438 pre-eruptive magmatic process prior to the 2006 explosive eruptions at Tungurahua volcano  
1439 (Ecuador). *J. Volcanol. Geotherm. Res.*, 199(1-2), 69-84. <https://doi.org/10.1016/j.jvolgeores.2010.10.010>  
1440  
1441  
1442 Sato, E. & Sato, H. (2009) Study of effect of magma pocket on mixing of two magmas with  
1443 different viscosities and densities by analogue experiments. *J. Volcanol. Geotherm. Res.*  
1444 *181(1-2)*, 115–123. <https://doi.org/10.1016/j.jvolgeores.2009.01.005>  
1445  
1446 Schleicher, J.M., Bergantz, G.W., Breidenthal, R.E. and Burgisser, A. (2016). Time scales of  
1447 crystal mixing in magma mushes. *Geophys. Res. Lett.*, 43(4), 1543-1550.  
1448 <https://doi.org/10.1002/2015GL067372>  
1449  
1450 Schleicher, J.M. & Bergantz, G.W. (2017). The mechanics and temporal evolution of an open  
1451 system magmatic intrusion into a crystal-rich magma. *J. Petrol.*, 58(6), 1059-1072.  
1452 <https://doi.org/10.1093/petrology/egx045>  
1453  
1454 Schubert, M., Driesner, T., Gerya, T. G. & Ulmer, P. (2013). Mafic injection as a trigger for  
1455 felsic magmatism: A numerical study. *Geochem. Geophys. Geosyst.*, 14(6), 1910-1928.  
1456 <https://doi.org/10.1002/ggge.20124>  
1457  
1458 Scott, J. A. J., Pyle, D., M., Mather, T. A., Rose, W. I. (2013). Geochemistry and evolution of  
1459 the Santiaguito volcanic dome complex, Guatemala. *J. Volcanol. Geotherm. Res.*, 252, 92-  
1460 107. <https://doi.org/10.1016/j.jvolgeores.2012.11.011>  
1461  
1462 Seitz, S., Putlitz, B., Baumgartner, L. P. & Bouvier, A. (2018). The role of crustal melting in  
1463 the formation of rhyolites: Constraints from SIMS oxygen isotope data (Chon Aike Province,  
1464 Patagonia, Argentina). *Am. Min.* 103(12), 2011-2027. <https://doi.org/10.2138/am-2018-6520>  
1465  
1466 Semenov, A. N. & Polyansky, O. P. (2017). Numerical modelling of the mechanisms of  
1467 magma mingling and mixing: A case study of the formation of complex intrusions. *Russ.*  
1468 *Geol. Geophys.*, 58(11), 1317-1332. <https://doi.org/10.1016/j.rgg.2017.11.001>

1469  
1470 Silva, M. M. V. G., Neiva, A. M. R. & Whitehouse, M. J. (2000). Geochemistry of enclaves  
1471 and host granites from the Nelas area, central Portugal. *Lithos*, 50(1-3), 153-170.  
1472 [https://doi.org/10.1016/S0024-4937\(99\)00053-5](https://doi.org/10.1016/S0024-4937(99)00053-5)  
1473  
1474 Sinton, J. M. & Detrick, R. S. (1992). Mid Ocean Ridge magma chambers. *J. Geophys. Res.*,  
1475 97(B1), 197-216. <https://doi.org/10.1029/91JB02508>  
1476  
1477 Snyder, D. (1997). The mixing and mingling of magmas. *Endeavour*, 21(1), 19-22.  
1478 [https://doi.org/10.1016/S0160-9327\(96\)10032-6](https://doi.org/10.1016/S0160-9327(96)10032-6)  
1479  
1480 Snyder, D. & Tait, S. (1995). Replenishment of magma chambers: a comparison of fluid me-  
1481 chanic experiments with field relations. *Contrib. Mineral. Petrol.*, 122(3), 230-240.  
1482 <https://doi.org/10.1007/s004100050123>  
1483  
1484 Solano, J. M. S., Jackson, M. D., Sparks, R. S. J. Blundy, J. D. & Annen, C. (2012). Melt  
1485 Segregation in Deep Crustal Hot Zones: a Mechanism for Chemical Differentiation, Crustal  
1486 Assimilation and the Formation of Evolved Magmas. *J. Petrol.*, 53(10), 1999-2026.  
1487 <https://doi.org/10.1093/petrology/egs041>  
1488  
1489 Sparks, R. S. J., Annen, C., Blundy, J. D., Cashman, K. V., Rust, A. C. and Jackson, M. D.  
1490 (2019). Formation and dynamics of magma reservoirs. *Phil. Trans. R. Soc. A.*, 377(2139),  
1491 20180019. <https://doi.org/10.1098/rsta.2018.0019>  
1492  
1493 Sparks, R. S. J. & Marshall, L. A. (1986). Thermal and mechanical constraints on mixing be-  
1494 tween mafic and silicic magmas. *J. Volcanol. Geotherm. Res.*, 29(1-4), 99-124.  
1495 [https://doi.org/10.1016/0377-0273\(86\)90041-7](https://doi.org/10.1016/0377-0273(86)90041-7)  
1496  
1497 Sparks, R. S. J., Sigurdsson, H. & Wilson, L. (1977). Magma mixing: a mechanism for trig-  
1498 gering acid explosive eruptions. *Nature*, 267, 315-318. <https://doi.org/10.1038/267315a0>  
1499  
1500 Spina, L., Cimarelli, C., Scheu, B., Di Genova, D., Dingwell, D. B. (2016). On the slow de-  
1501 compressive response of volatile- and crystal-bearing magmas: An analogue experimental in-  
1502 vestigation. *Earth Planet. Sci. Lett.*, 433, 44-53. <https://doi.org/10.1016/j.epsl.2015.10.029>  
1503  
1504 Stelten, M. E., Cooper, K. M., Vazquez, J. A., Calvert, A. T. & Glessner, J. J. G. (2015).  
1505 Mechanisms and Timescales of Generating Eruptible Magmas at Yellowstone Caldera from  
1506 Zircon and Sanidine Geochronology and Geochemistry. *J. Petrol.*, 56(8), 1607-1642.  
1507 <https://doi.org/10.1093/petrology/egv047>  
1508  
1509 Tepley, F. J., Davidson, J. P. & Clyne, M. A. (1999). Magmatic Interactions as Recorded in  
1510 Plagioclase Phenocrysts of Chaos Crags, Lassen Volcanic Centre, California. *J. Petrol.*,  
1511 40(5), 787-809. <https://doi.org/10.1093/ptroj/40.5.787>  
1512  
1513 Thomas, N. & Tait, S. (1997). The dimensions of magmatic inclusions as a constraint on the  
1514 physical mechanism of mixing. *J. Volcanol. Geotherm. Res.*, 75, 167-178.  
1515 [https://doi.org/10.1016/S0377-0273\(96\)00034-0](https://doi.org/10.1016/S0377-0273(96)00034-0)  
1516

1517 Thomas, N., Tait, S. & Koyaguchi, T. (1993). Mixing of stratified liquids by the motion of  
1518 gas bubbles: application to magma mixing. *Earth Planet. Sci. Lett.*, *115*(1-4), 161-175.  
1519 [https://doi.org/10.1016/0012-821X\(93\)90220-4](https://doi.org/10.1016/0012-821X(93)90220-4)  
1520

1521 Topley, C. G., Brown, M., D'Lemos, R. S., Power, G. M. & Roach, R. A. (1990). The North-  
1522 ern Igneous Complex of Guernsey, Channel Islands. *Geol. Soc. Spec. Pub.*, *51*, 245-259.  
1523 <https://doi.org/10.1144/GSL.SP.1990.051.01.15>  
1524

1525 Troll, V. R. & Schmicke, H. (2002). Magma Mixing and Crustal Recycling Recorded in Ter-  
1526 nary Feldspar from Compositionally Zoned Peralkaline Ignimbrite 'A', Gran Canaria, Canary  
1527 Islands. *J. Petrol.*, *43*(2), 243-270. <https://doi.org/10.1093/petrology/43.2.243>  
1528

1529 Tsuchiyama, A. (1985). Dissolution kinetics of plagioclase in the melt of the system diop-  
1530 side-albite-anorthite, and the origin of dusty plagioclase in andesites. *Contrib. Mineral. Pet-  
1531 rol.*, *89*(1), 1-16. <https://doi.org/10.1007/BF01177585>  
1532

1533 Tsuchiyama, A. & Takahashi, E., 1983. Melting kinetics of a plagioclase feldspar. *Contrib.  
1534 Mineral. Petrol.*, *84*(4), 345-354. <https://doi.org/10.1007/BF01160286>  
1535

1536 Ubide, T., Galé, C., Larrea, P., Arranz, E. & Lago, M. (2014). Antecrysts and their effect on  
1537 rock compositions: The Cretaceous lamprophyre suite in the Catalonian Coastal Ranges (NE  
1538 Spain). *Lithos*, *206-207*, 214-233. <https://doi.org/10.1016/j.lithos.2014.07.029>  
1539

1540 Ubide, T., Galé, C., Larrea, P., Arranz, E., Lago, M. & Tierz, P. (2014). The Relevance of  
1541 Crystal Transfer to Magma Mixing: a Case Study in Composite Dykes from the Central Pyre-  
1542 nees. *J. Petrol.*, *55*(8), 1535-1559. <https://doi.org/10.1093/petrology/egu033>  
1543

1544 Van der Laan, S. R. & Wyllie, P. J. (1993). Experimental Interaction of Granitic and Basaltic  
1545 Magmas and Implications for Mafic Enclaves. *J. Petrol.*, *34*(3), 491-517.  
1546 <https://doi.org/10.1093/petrology/34.3.491>  
1547

1548 Van Zalinge, M. E., Sparks, R. S. J., Cooper, F. J. and Condon, D. J. (2016). Early Miocene  
1549 large-volume ignimbrites of the Oxaya Formation, Central Andes. *J. Geol. Soc.*, *173*(5), 716-  
1550 733. <https://doi.org/10.1144/jgs2015-123>  
1551

1552 Venezky, D. Y. & Rutherford, M. J. (1999). Petrology and Fe-Ti oxide reequilibration of the  
1553 1991 Mount Unzen mixed magma. *J. Volcanol. Geotherm. Res.*, *89*(1-4), 213-230.  
1554 [https://doi.org/10.1016/S0377-0273\(98\)00133-4](https://doi.org/10.1016/S0377-0273(98)00133-4)  
1555

1556 Vernon, R. H. (1990). Crystallization and Hybridism in Microgranitoid Enclave Magmas:  
1557 Microstructural Evidence. *J. Geophys. Res.*, *95*(B11), 17849-17859.  
1558 <https://doi.org/10.1029/JB095iB11p17849>  
1559

1560 Vetere, F., Petrelli, M., Morgavi, D. & Perugini, D. (2015). Dynamics and time evolution of a  
1561 shallow plumbing system: The 1739 and 1888-90 eruptions, Vulcano Island, Italy. *J. Vol-  
1562 canol. Geotherm. Res.*, *306*, 74-82. <https://doi.org/10.1016/j.jvolgeores.2015.09.024>  
1563

1564 Vogel, T. A., Hidalgo, P. J., Patino, L., Tefend, K. S. & Ehrlich, R. (2008), Evaluation of  
1565 magma mixing and fractional crystallization using whole-rock chemical analyses: Polytopic

1566 vector analyses, *Geochem. Geophys. Geosyst.*, 9(4), Q04020.  
1567 <https://doi.org/10.1029/2007GC001790>  
1568  
1569 Wada, H., Harayama, S. & Yamaguchi, Y. (2004). Mafic enclaves densely concentrated in  
1570 the upper part of a vertically zoned felsic magma chamber: The Kurobegawa granitic pluton,  
1571 Hida Mountain Range, central Japan. *Geol. Soc. Am. Bull.*, 116(7-8), 788-801.  
1572 <https://doi.org/10.1130/B25287.1>  
1573  
1574 Wadge, G., Voight, B., Sparks, R. S. J., Cole, P. D., Loughlin, S. C. & Robertson, R. E. A.  
1575 (2014). An overview of the eruption of Soufrière Hills Volcano, Montserrat from 2000 to  
1576 2010. *Geol. Soc. Lond. Mem.*, 39, 1-40. <https://doi.org/10.1144/M39.1>  
1577  
1578 Watson, E.B. (1982) Basaltic contamination by continental crust: some experiments and  
1579 models. *Contrib. Mineral. Petrol.*, 80(1), 73–87. <https://doi.org/10.1007/BF00376736>  
1580  
1581 Watson, E. B. & Jurewicz, S. R. (1984). Behavior of alkalis during diffusive interaction of  
1582 granitic xenoliths with basaltic magma. *J. Geol.*, 92(2), 121-131.  
1583 <https://doi.org/10.1086/628843>  
1584  
1585 Weidendorfer, D., Mattsson, H. B. & Ulmer, P. (2014). Dynamics of Magma Mixing in Par-  
1586 tially Crystallised Magma Chambers: Textural and Petrological Constraints from the Basal  
1587 Complex of the Austurhorn Intrusion (SE Iceland). *J. Petrol.*, 55(9), 1865-1903.  
1588 <https://doi.org/10.1093/petrology/egu044>  
1589  
1590 Wiebe, R. A. (1973). Relations between coexisting basaltic and granitic magmas in a compo-  
1591 site dike. *Am. J. Sci.*, 273, 130-151.  
1592  
1593 Wiebe, R. A. (1992). The Pleasant Bay Layered Gabbro-Diorite, Coastal Maine: Ponding and  
1594 Crystallization of Basaltic Injections into a Silicic Magma Chamber. *J. Petrol.*, 34(3), 461-  
1595 489. <https://doi.org/10.1093/petrology/34.3.461>  
1596  
1597 Wiebe, R. A. (1994). Silicic Magma Chambers as Traps for Basaltic Magmas: The Cadillac  
1598 Mountain Intrusive Complex, Mount Desert Island, Maine. *J. Geol.*, 102(4), 423-437.  
1599 <https://doi.org/10.1086/629684>  
1600  
1601 Wiebe, R. A. (1996) Mafic-silicic layered intrusions: the role of basaltic injections on mag-  
1602 matic processes and the evolution of silicic magma chambers. *Trans. R. Soc. Edinburgh*  
1603 *Earth Sci.*, 87(1-2), 233-242. <https://doi.org/10.1017/S0263593300006647>  
1604  
1605 Wiebe, R. A. & Collins, W. J. (1998). Depositional features and stratigraphic sections on gra-  
1606 nitic plutons: implications for the emplacement and crystallization of granitic magma. *J.*  
1607 *Struct. Geol.*, 20(9-10), 1273-1289. [https://doi.org/10.1016/S0191-8141\(98\)00059-5](https://doi.org/10.1016/S0191-8141(98)00059-5)  
1608  
1609 Wiebe, R. A., Blair, K. D., Hawkins, D. P. & Sabine, C. P. (2002). Mafic injections, in situ  
1610 hybridization, and crystal accumulation in the Pyramid Peak granite, California. *GSA Bull.*,  
1611 114(7), 909-920. [https://doi.org/10.1130/0016-7606\(2002\)114%3C0909:MII-](https://doi.org/10.1130/0016-7606(2002)114%3C0909:MII-SHA%3E2.0.CO;2)  
1612 [SHA%3E2.0.CO;2](https://doi.org/10.1130/0016-7606(2002)114%3C0909:MII-SHA%3E2.0.CO;2)  
1613

1614 Wiebe, R. A. & Hawkins, D. P. (2015). Growth and Impact of a Mafic-Silicic Layered Intrusion in the Vinalhaven Intrusive Complex, Maine. *J. Petrol.*, 56(2), 273-298.  
1615 <https://doi.org/10.1093/petrology/egu078>  
1616  
1617  
1618 Wiebe, R. A., Smith, D., Sturm, M., King, E. M. & Seckler, M. S. (1997). Enclaves in the  
1619 Cadillac Mountain Granite (Coastal Maine): Samples of Hybrid Magma from the Base of the  
1620 Chamber. *J. Petrol.*, 38(3), 393-423. <https://doi.org/10.1093/etroj/38.3.393>  
1621  
1622 Wiesmaier, S., Morgavi, D., Renggli, C. J., Perugini, D., De Campos, C. P., Hess, K. U., Ertel-Ingrisch, W., Lavallée, Y. & Dingwell, D. B. (2015). Magma mixing enhanced by bubble  
1623 segregation. *Solid Earth*, 6, 1007-1023. <https://doi.org/10.5194/se-6-1007-2015>  
1624  
1625  
1626 Wilcox, R. (1999). The Idea of Magma Mixing: History of a Struggle for Acceptance. *J. Geol.*, 107(4), 421-432. <https://doi.org/10.1086/314357>  
1627  
1628  
1629 Williams, Q. & Tobisch, O. T. (1994). Microgranitic enclave shapes and magmatic strain histories: Constraints from drop deformation theory. *J. Geophys. Res.*, 99(B12), 24359-24368.  
1630 <https://doi.org/10.1029/94JB01940>  
1631  
1632  
1633 Woods, A. W. & Stock, M. J. (2019). Some fluid mechanical constraints on crystallization and recharge within sills. *Phil. Trans. R. Soc. A.*, 377, 20180007.  
1634 <http://dx.doi.org/10.1098/rsta.2018.0007>  
1635  
1636  
1637 Wright, H. M. N., Folkes, C. B., Cas, R. A. F. and Cashman, K. V. (2011). Heterogeneous pumice populations in the 2.08-Ma Cerro Galán Ignimbrite: implications for magma recharge and ascent preceding a large volume silicic eruption. *Bull. Volcanol.*, 73(10), 1513-1533.  
1638 <https://doi.org/10.1007/s00445-011-0525-5>  
1639  
1640  
1641  
1642 Xiong, F., Ma, C., Zhang, J. & Liu, B. (2012). The origin of mafic microgranular enclaves and their host granodiorites from East Kunlun, Northern Qinghai-Tibet Plateau: implications for magma mixing during subduction of Paleo-Tethyan lithosphere. *Mineral. Petrol.*, 104(3-4), 211-224. <https://doi.org/10.1007/s00710-011-0187-1>  
1643  
1644  
1645  
1646  
1647 Zhang, J., Davidson, J. P., Humphreys, M. C. S., Macpherson, C. G. & Neill, I. (2015). Magmatic Enclaves and Andesite Lavas from Mt. Lamington, Papua New Guinea: Implications for Recycling of Earlier-fractionated Minerals through Magma Recharge. *J. Petrol.*, 56(11), 2223-2256. <https://doi.org/10.1093/petrology/egv071>  
1648  
1649  
1650

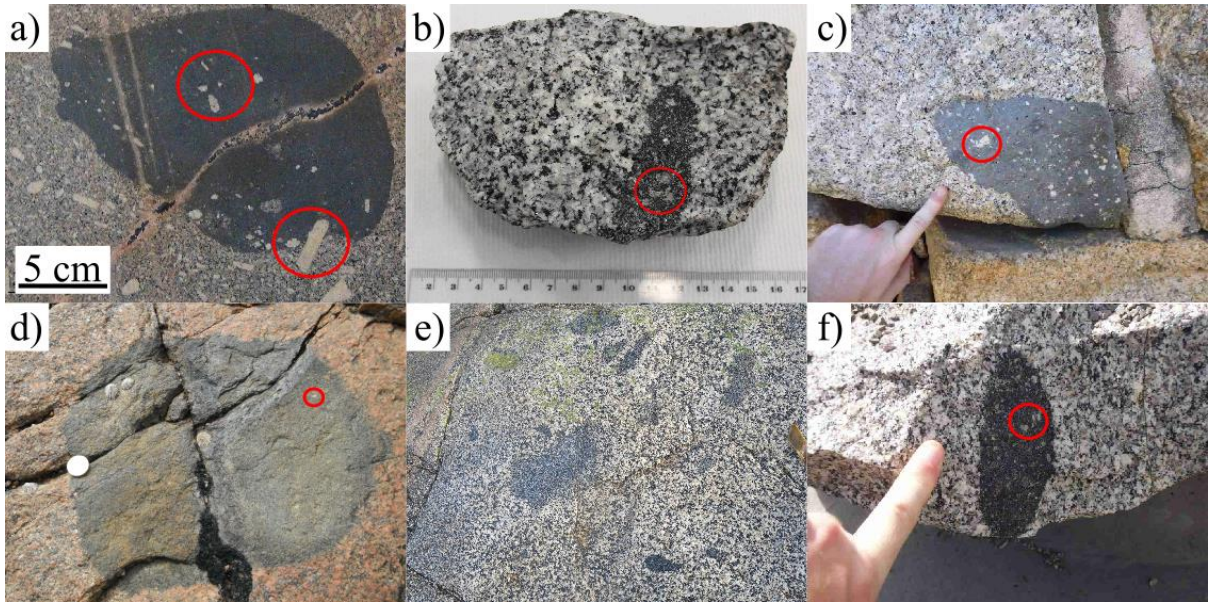


Figure 1: Examples of mafic enclaves. All are generally finer grained than their hosts but contain occasional large crystals (circled in red), which are xenocrysts mechanically transferred from the host. a) Large ( $\approx 18$  cm) fine-grained enclave hosted in alkali-feldspar granite from Blackenstone Quarry, Dartmoor, England. b) High aspect ratio enclave from the Adamello Massif, Italy. c) Mafic enclave in granite of stone wall at Hiroshima Castle, Japan. d) Mafic enclave within the Cobo Granite, Guernsey. e) Numerous enclaves in an outcrop of the Northern Igneous Complex, Guernsey. The outcrop shown is about  $1 \text{ m}^2$ . f) Mafic enclave in a granite statue in Alexander Garden, Moscow.

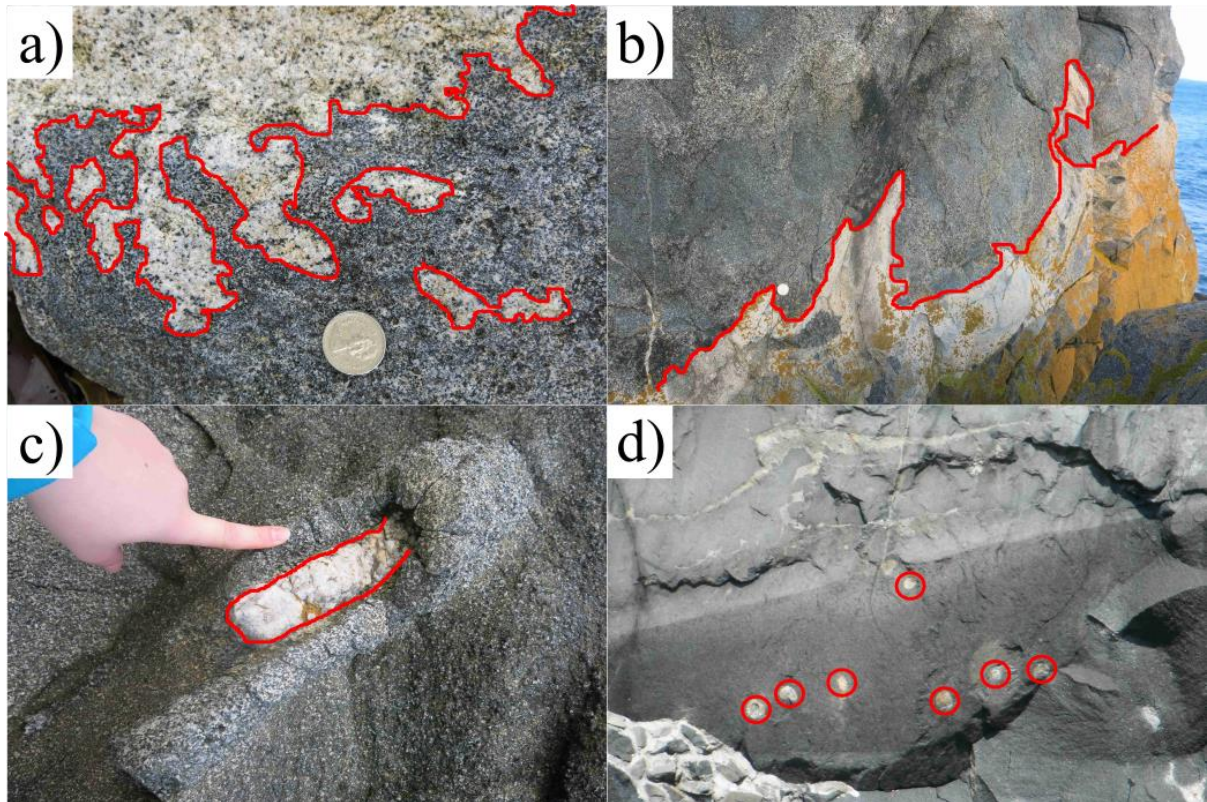


Figure 2: Examples of mingling textures from layered intrusions of the Northern Igneous Complex, Guernsey. Noted textures are outlined in red. a) Loose block showing intimate mingling between a felsic and a mafic magma. b) Diapir-like structures of felsic material rising into a mafic layer. c) Pipe of felsic material penetrating a mafic layer. d) Cross section through pipes similar to that seen in c).

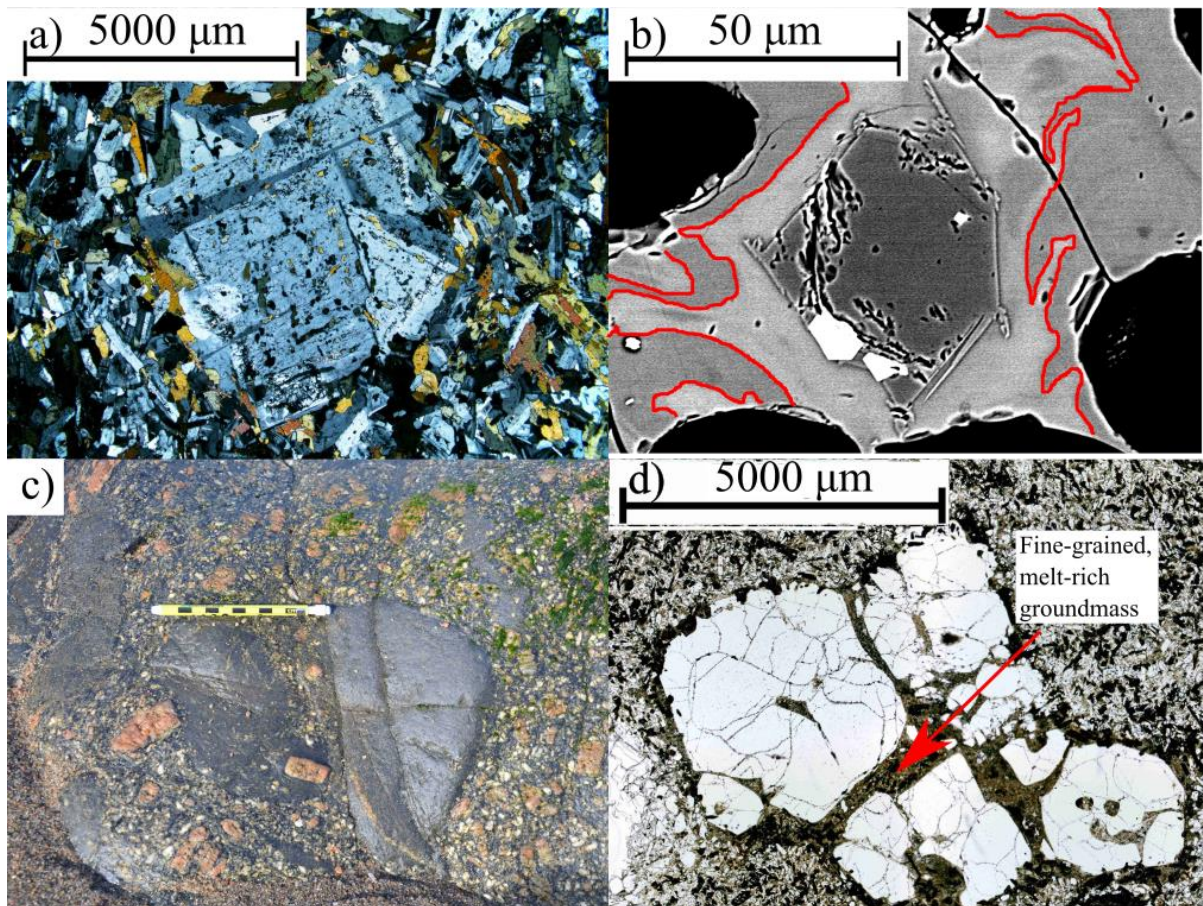


Figure 3: Examples of magmatic xenocrysts. a) Plagioclase xenocryst in a mafic enclave from the Adamello Massif, Italy, showing a sieved core with many inclusions of hornblende. b) Back-scatter electron (BSE) image of an olivine xenocryst in an andesitic lava flow from White Island volcano, New Zealand. The crystal is surrounded by an irregular film of basaltic glass (bounded by red contour). Image courtesy of Geoff Kilgour. c) Alkali feldspar xenocrysts, up to 3 cm, within mafic rocks on Shetland, Scotland. The relation of the mafic rocks to the felsic rocks from which the feldspars originated is unknown since the contact is in the subsurface. Image courtesy of Amy Gilmer. d) A cluster of rounded and highly fractured quartz xenocrysts in the Cardones ignimbrite, Chile (van Zalinge et al., 2016). The surrounding groundmass is much finer-grained and melt-rich than the rest of the material. The cluster has a rim of opaque crystals.

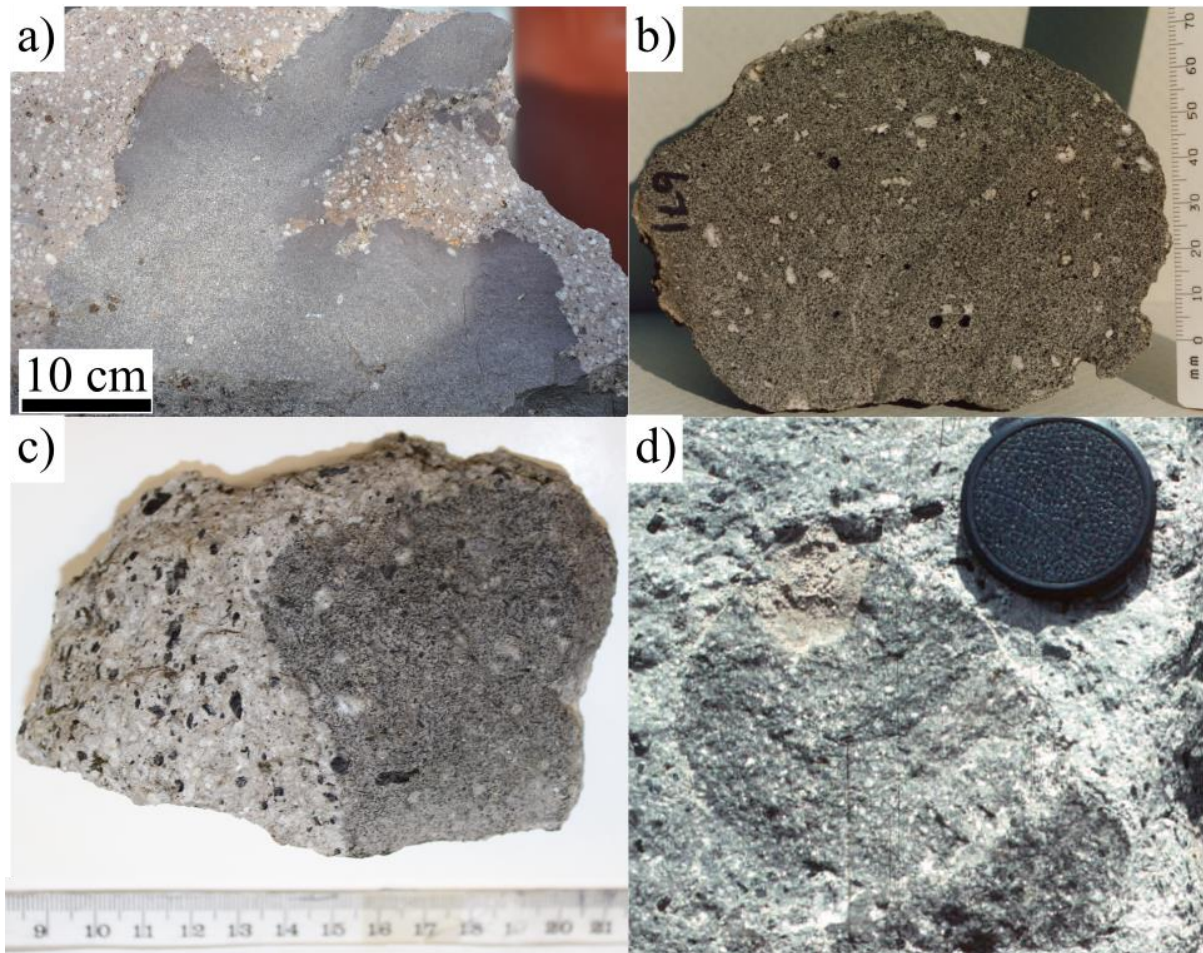


Figure 4: Examples of enclaves from four volcanic systems. a) Mafic enclave, with fine-grained, crenulate margin and numerous xenocrysts, from Chaos Crags. Image courtesy of Michael Clynné. b) Andesitic enclave from 1915 eruption of Lassen Peak, showing an equigranular texture and numerous partially reacted xenocrysts. Reproduced with permission from Clynné (1999). c) Basaltic enclave in an andesitic lava flow from the 1792 dome collapse at Mt. Unzen, Japan, at about 4 ka. There is no evidence for a fine-grained margin in the enclave. Sample collected by Julie Oppenheimer, Karen Strehlow and Emma Liu. d) Mafic enclave from 1995-2010 eruption of Soufrière Hills volcano. Image courtesy of Steve Sparks.

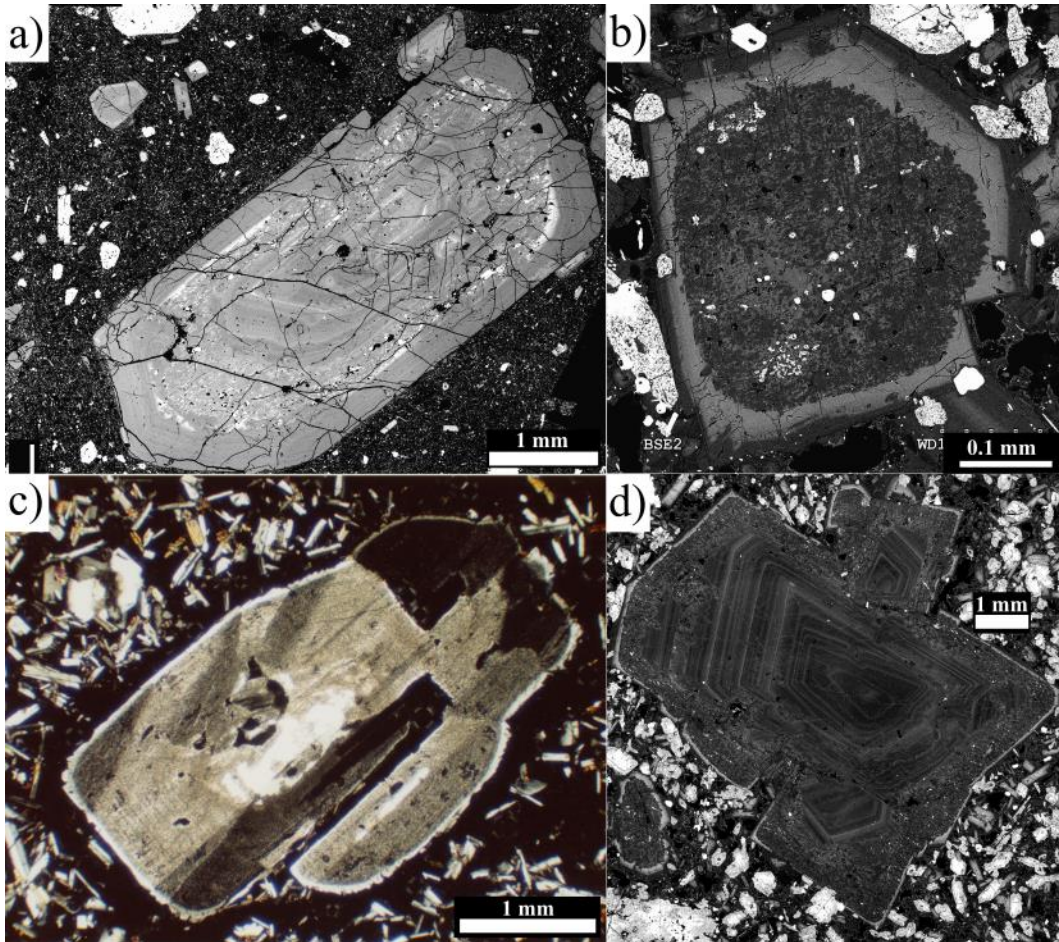


Figure 5: BSE images of plagioclase phenocrysts and xenocrysts from Mt. Unzen (a, b, d) and Lassen Peak (c). a) Host-rock plagioclase phenocryst with a wide heterogeneous zone and many mineral and glass inclusions. b) Plagioclase xenocryst in an enclave with a sieved core. c) Heavily reacted plagioclase xenocryst with a clear overgrowth rim within an andesitic enclave. Reproduced with permission from Clynne (1999). d) Plagioclase xenocryst in a mafic enclave with an oscillatory zoned core surrounded by a patchily zoned and including-rich mantle bounded by a normally-zoned rim.

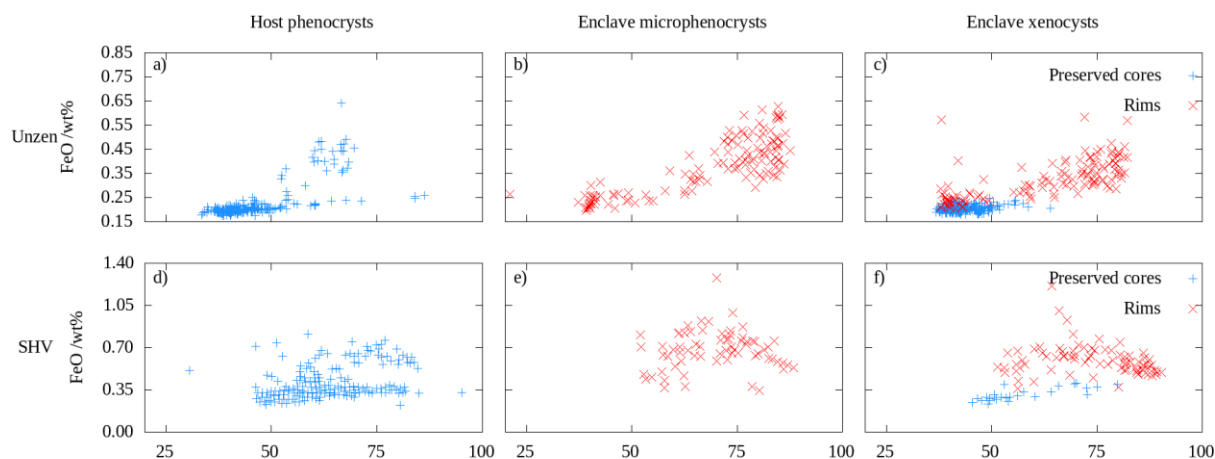


Figure 6: Plots of FeO versus An from transects across plagioclase for a,d) host phenocrysts, b,e) enclave microphenocrysts from and c,f) xenocrysts in enclaves. Data shown for Mt. Unzen sample in Fig. 4c and for rocks from Soufrière Hills (Humphreys et al., 2009). a,d) Most host phenocrysts lie on a shallow, linear trend with slight positive correlation in the range An = 33-88 mol% for Mt. Unzen and An = 45 – 80 mol% for Soufrière Hills. Some analyses show much greater FeO enrichment and correspond to resorbed zones. b,e) Enclave microphenocrysts show FeO enrichment compared to host phenocrysts, up to 0.65 wt% for Mt. Unzen and 1.3 wt% for Soufrière Hills. c,f) The preserved cores of xenocrysts plot on the same shallow trend as host phenocrysts whilst rim compositions overlap with enclave microphenocryst compositions.

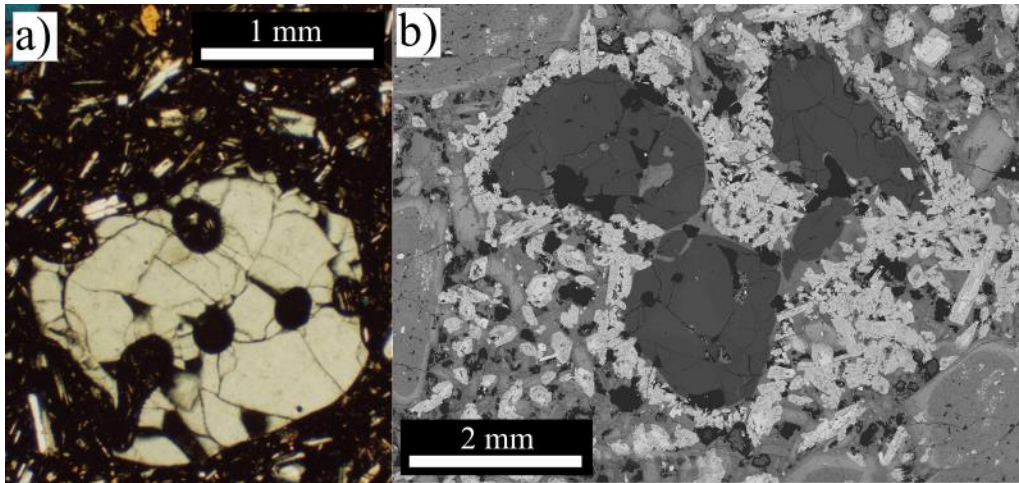


Figure 7: a) Image of a quartz phenocryst in the dacitic lava dome from the 1915 Lassen Peak eruption. It appears unreacted but has rounded edges and embayments. Image courtesy of Michael Clynne. b) BSE image of a cluster of quartz xenocrysts in an enclave from the 1991-1995 Mt. Unzen eruption. They are rounded and surrounded by an extended region of hornblende microphenocrysts (very bright), glass (light grey) and vesicle (black).

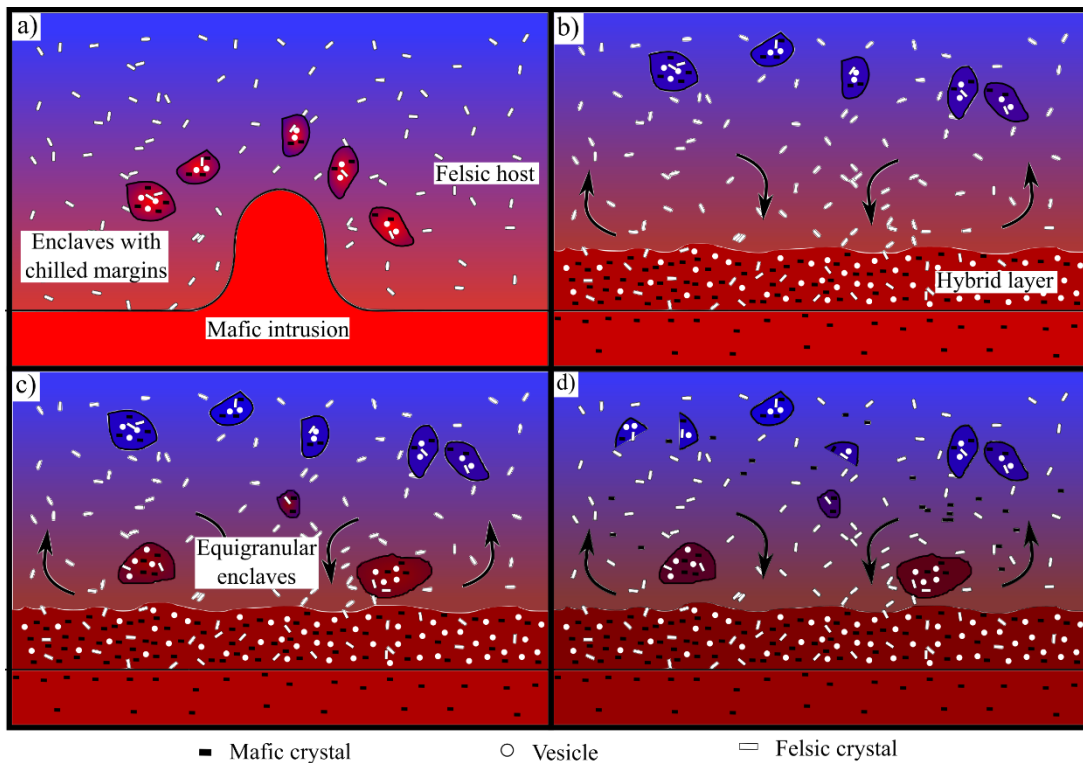


Figure 8: Conceptual model of the different stages of magma mixing and mingling following injection of a mafic magma into a partially crystallised silicic host. The processes shown follow similar diagrams from Clyne (1999), Tepley et al. (1999), Browne et al. (2006) and Plail et al. (2014). a) Mafic magma is injected into a partially crystallised host. Injected magma is initially denser and so ponds beneath the silicic host, although the momentum of the injection may produce a collapsing fountain. b) Disaggregation of the collapsing fountain produces quenched enclaves with chilled margins. These enclaves contain xenocrysts captured from the host, which became entrained during the injection. Heat transfer from the mafic to the silicic magma produces partial melting of the silicic member, reducing the crystallinity and creating convective motions that disperse the enclaves. Additionally, a hybrid layer forms at the interface between the mafic and silicic magmas. Crystallisation in this layer leads to exsolution of volatile phases. c) The presence of exsolved volatiles in the interface layer leads to a reduction in density and the hybrid layer destabilises due to a Rayleigh-Taylor instability. This leads to the formation of enclaves without chilled margins that are dispersed within the silicic host. d) Continued convective motions in the host lead to brittle disaggregation of enclaves creating angular enclave fragments, and dispersing mafic ground-mass and resorbed host crystals into the host.